AD-A097 712 BOSTON COLL CHESTNUT HILL MA SPACE DATA ANALYSIS LAB F/G 4/1
IONOSPHERIC ELECTRON DENSITY PROFILE AND RELATED STUDIES.(U)
FEB 81 B BASU, T S CHANG, E R SMITH F19628-77-C-0243
UNCLASSIFIED BC-SDAL-81-1 AFGL-TR-81-0021 NL

1 OF 1
AD A 097 712

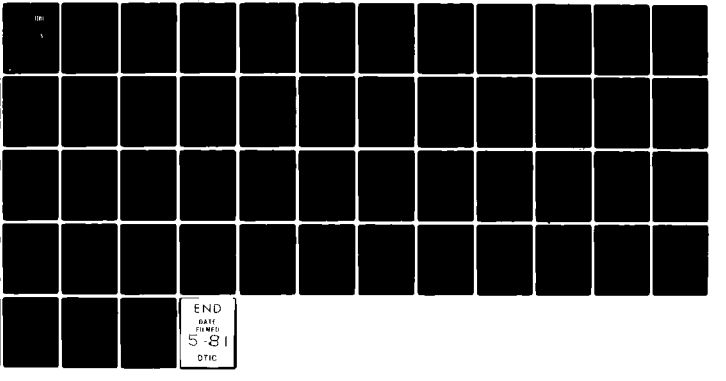

AFGL-TR-81-0021

(12)

IONOSPHERIC ELECTRON DENSITY PROFILE AND RELATED STUDIES

LEVEL II

Bamandas Basu
Tien S. Chang
Ed R. Smith

Space Data Analysis Laboratory
Boston College
Chestnut Hill, Massachusetts 02167

AD A097712

DTIC
ELECTE
APR 14 1981
S
E

Final Report
22 November 1977 - 30 September 1980

Approved for Public Release, Distribution Unlimited

Air Force Geophysics Laboratory
Air Force Systems Command
United States Air Force
Hanscom AFB, Massachusetts 01731

DTIC FILE COPY

81 4 14 .31

UNCLASSIFIED

SECURITY CLASSIFICATION OF THIS PAGE (When Data Entered)

REPORT DOCUMENTATION PAGE	READ INSTRUCTIONS BEFORE COMPLETING FORM
1. REPORT NUMBER: AFGL-TR-81-0021	2. GOVT ACCESSION NO.: AD-A097 772
	3. RECIPIENT'S CATALOG NUMBER:
4. TITLE (and Subtitle): IONOSPHERIC ELECTRON DENSITY PROFILE AND RELATED STUDIES	5. TYPE OF REPORT & PERIOD COVERED: Final Report 22 Nov 77 - 30 Sep 80
	6. PERFORMING ORG. REPORT NUMBER: BC-SDAL-81-1
7. AUTHOR(s): Bamandas Basu, S. Chang, Ed R. Smith	8. CONTRACT OR GRANT NUMBER(s): F19628-77-C-0243
9. PERFORMING ORGANIZATION NAME AND ADDRESS: Trustees of Boston College, Chestnut Hill, Massachusetts 02167	10. PROGRAM ELEMENT, PROJECT, TASK AREA & WORK UNIT NUMBERS: 62101F, 192455AA, 17 55
11. CONTROLLING OFFICE NAME AND ADDRESS: Air Force Geophysics Laboratory, Hanscom AFB, Massachusetts 01731, Contract Monitor/Dr. John Jasperse/PHI	12. REPORT DATE: 3 February 1981
	13. NUMBER OF PAGES: 57
14. MONITORING AGENCY NAME & ADDRESS (if different from Controlling Office)	15. SECURITY CLASS. (of this report): Unclassified
	15a. DECLASSIFICATION DOWNGRADING SCHEDULE

16. DISTRIBUTION STATEMENT (of this Report)

Approved for Public Release; Distribution Unlimited

17. DISTRIBUTION STATEMENT (of the abstract entered in Block 20, if different from Report)

18. SUPPLEMENTARY NOTES

19. KEY WORDS (Continue on reverse side if necessary and identify by block number)

Boltzmann-Fokker-Planck Theory
Collision Operators
Electron Cyclotron Instability
Electron Energy Distribution
Electrostatic Plasma Instabilities
Energy Deposition Rate
Kinetic Equation
Precipitating Fluxes
Upper Hybrid Instability

20. ABSTRACT (Continue on reverse side if necessary and identify by block number)

There are many problems of practical interest in the study of the Earth's ionosphere that require a detailed knowledge of the electron energy distribution and the electron density profile. This report summarizes our theoretical efforts in explaining the observed electron distribution functions. Boltzmann-Fokker-Planck theory has been used, and the resulting kinetic equation has been analyzed. A systematic study of the collision operators that appear in the kinetic equation has been done. Electrostatic plasma instabilities have been (Cont.)

DD FORM 1 JAN 73 1473

UNCLASSIFIED 403460

SECURITY CLASSIFICATION OF THIS PAGE (When Data Entered)

20. Abstract (Cont.)

investigated in order to explain the observed anomalous structure of the electron energy distribution in the 2-4 eV range. In a related study, the problem of auroral proton precipitation has been solved analytically. This analysis enables us to calculate the precipitating proton-hydrogen fluxes, energy deposition rate, and the electron density profile resulting from ionization.

ACKNOWLEDGEMENTS

The authors wish to thank Mr. Leo F. Power, Jr., the Director of the Space Data Analysis Laboratory, for his able administrative assistance throughout the duration of this contract.

Special thanks go to Mr. Neil Grossbard of the laboratory for his programming and analysis efforts.

To the Contract Monitor, Dr. J. R. Jasperse thanks are extended for his collaboration and assistance.

We wish to thank Miss Mary Kelly for an excellent job in typing this document.

TABLE OF CONTENTS

TABLE OF CONTENTS (Cont.)

1 BACKGROUND

In the study of the Earth's ionosphere, there are many problems that require a detailed knowledge of the electron distribution function. The electrons are produced primarily by the photoionization of the neutral particles in the atmosphere by the electromagnetic radiation from the sun, and by secondary impact ionization of the atmospheric constituents by the primary electrons. The electrons undergo various collisional interactions with the atmospheric particles and a steady-state distribution is reached. In the auroral atmosphere, ionization can also result from the precipitation of the high energy (keV) electrons and protons. Once the electron distribution function is determined, ionospheric properties of interest can then be calculated. With the advent of rocket-borne and satellite electron spectrometers it is of interest to pursue detailed theoretical studies of the photoelectron distribution as well as of the electron density profile in the auroral ionosphere.

The Space Data Analysis Laboratory (SDAL) of Boston College was contracted by the Ionospheric Dynamics Branch (PHI) of the Air Force Geophysics Laboratory (AFGL) to develop analytic and computer techniques for theoretical studies of the ionospheric electron distribution function. This report is a summary of the work performed under the auspices of SDAL during the period covered by the contract.

2 PHOTOELECTRON FLUX IN EARTH'S IONOSPHERE AT ENERGIES NEAR THE PHOTOIONIZATION PEAKS

In this work Boltzmann-Fokker-Planck (BFP) theory is used to analyze the (isotropic) photoelectron flux in the Earth's ionosphere at energies in the vicinity of photoionization peaks, where the electron impact cross-sections are slowly varying functions of energy.

2.1 GREEN'S FUNCTION SOLUTION FOR THE PHOTOELECTRON FLUX

In the steady-state, local approximation an equation for the isotropic part of the electron distribution function is obtained by integrating the BFP equation over the angles in velocity space. The equation in the energy representation is

$$0 = \left(\frac{\delta F_o}{\delta t}\right)_{pi} + \left(\frac{\delta F_o}{\delta t}\right)_{coll} \quad , \tag{1}$$

where the terms on the right-hand side are given by Eqs. (7) through (15) of Jasperse (1976) and in Jasperse (1975). At energies in the vicinity of photoionization peaks the momentum transfer, excitation, and ionization cross-sections are slowly varying functions of energy and, as a result, this equation may be approximated by

$$\left[-a \frac{d^2}{dE^2} - b \frac{d}{dE} + c\right] H(E) = S(E) \quad , \tag{2}$$

where H is 1_m times the isotropic part of the electron distribution function divided by $E^{1/2}$, and where

$$a = \frac{Y_{ee}\, n_e\, T_e}{2} + \left(\frac{2}{m}\right)^{1/2} \sum_j \delta_j\, n_j < E^2 Q_{mnj}(E) > T_n \quad ,$$

$$b = \frac{Y_{ee}\, n_e}{2} + \left(\frac{2}{m}\right)^{1/2} \sum_j \delta_j\, n_j < E^2 Q_{mnj}(E) > \quad ,$$

$$c = \left(\frac{2}{m}\right)^{1/2} \sum_{jk} n_j < E Q_{jk}(E) >$$

$$+ \left(\frac{2}{m}\right)^{1/2} \sum_{jk} n_j < E Q_{ijk}(E) > \quad ,$$

$$Y_{ee} \equiv 16\pi(e^2/m)^2 \ln \Lambda \, (m/2)^3 \quad .$$

Here, Q_{mnj} are the momentum transfer cross sections, Q_{jk} are the impact excitation cross sections for electronic transitions, Q_{ijk} are the impact ionization cross sections, $\delta_j \equiv 2m/M_j$ where m is the electron mass and M_j is the neutral particle mass, and ln Λ is the Coulomb logarithm. The neutral particle densities are denoted by n with an appropriate subscript denoting the type and state of the neutral particle, the neutral particle temperature by T_n (in eV), and n_e and T_e denote the analagous electron quantities. The angular brackets denote an energy average. In deriving Eq. (2) rotational, vibrational, fine structure, electron-ion, de-excitation and recombination processes were found to be negligible. The production of secondary electrons by electron impact ionization was regarded as a known source by using the continuous slowing-down approximation and was included in S. In treating impact excitation of the electronic states, terms of the form

$$- \left(\frac{2}{m}\right)^{1/2} \sum_{jk} n_j < (E+\Delta_{jk}) \, Q_{jk}(E+\Delta_{jk}) > H(E+\Delta_{jk}) \quad ,$$

where Δ_{jk} are the threshold energies, were also neglected. It is actually possible to solve Eq. (2) with these terms included using mathematical methods more general than the ones presented in this paper. These terms produce approximately a 5% effect at energies in the vicinity of a peak produced only by photoionization. These more general results will be published elsewhere.

Eq. (2) can be solved if we are able to find the Green's functions which satisfies

$$\left[-a \frac{d^2}{dE^2} - b \frac{d}{dE} + c\right] G(E,E') = \delta(E-E') \quad , \tag{3}$$

subject to appropriate boundary conditions. Here, $\delta(E-E')$ is the Dirac delta function. The photoelectron flux, $\Phi(E)$, is then given by

$$\Phi(E) = (4\pi)^{-1} \left(\frac{2}{m}\right)^{1/2} E \int_0^\infty dE' \, G(E,E') \, S(E') \quad . \tag{4}$$

Using standard methods we obtain

$$G(E,E') = \frac{1}{a(\alpha_1+\alpha_2)} \begin{cases} \exp\left[+\alpha_2(E-E')\right] & , \quad E<E' \quad , \\ \exp\left[-\alpha_1(E-E')\right] & , \quad E>E' \quad . \end{cases} \tag{5}$$

where the boundary conditions that $G \to 0$ as $E \to \infty$ and that G have no rising solution as $E \to 0$, have been imposed. Here

$$\alpha_1 = \frac{1}{2a}\left(b^2+4ac\right)^{1/2} + \frac{b}{2a} \quad , \tag{6}$$

$$\alpha_2 = \frac{1}{2a}\left(b^2+4ac\right)^{1/2} - \frac{b}{2a} \quad . \tag{7}$$

2.1.1 Two Photoelectron Sources

The first photoelectron source we examine is that due to a continuously decreasing source and an isolated unbroadened photoionization source.

$$S(E) = S_o \exp(-E/E_o) + S_1 \delta(E-E_1) \quad . \tag{8}$$

Using Eq. (4), the photoelectron flux is

$$\Phi(E) = (4\pi)^{-1}\left(\frac{2}{m}\right)^{1/2} \frac{E}{a(\alpha_1+\alpha_2)}\left\{S_o f_o(E) + S_1 f_1(E)\right\}, \tag{9}$$

$$f_o(E) = \left[\frac{1}{(\alpha_1-1/E_o)} + \frac{1}{(\alpha_2+1/E_o)}\right]\exp(-E/E_o) - \frac{\exp(-\alpha_1 E)}{(\alpha_1-1/E_o)} \quad , \tag{10}$$

$$f_1(E) = \begin{cases} \exp\left[\alpha_2(E-E_1)\right] & , \quad E<E_1 \quad , \\ \exp\left[-\alpha_1(E-E_1)\right] & , \quad E>E_1 \quad . \end{cases} \tag{11}$$

Above about 260 km electron-neutral particle collisions are decreasing rapidly and electron-electron collisions dominate. This implies that $b^2 \gg 4ac$ and that $\alpha_1 \approx 1/T_e \approx \alpha_2 \approx 2c/Y_{ee}n_e$. Since the continous source decreases slowly $\alpha_1 \gg 1/E_o$; an approximate solution is

$$\Phi(E) \simeq (4\pi)^{-1} \left(\frac{2}{m}\right)^{1/2} \frac{2E}{Y_{ee} n_e} \left\{ \frac{S_o}{(2c/Y_{ee} n_e + 1/E_o)} \times \exp(-E/E_o) \right.$$

$$\left. + S_1 \begin{cases} \exp\left[2c(E-E_1)/Y_{ee} n_e\right], & E < E_1 \\ \exp\left[-(E-E_1)/T_e\right], & E > E_1 \end{cases} \right\} \quad (12)$$

At high altitudes we see that the photoelectron flux has a cusp at E_1 and a line shape that is asymmetric about E_1. The forward and backward half widths at the 1/e point are

$$FHW = T_e \quad , \quad (13)$$

$$BHW = Y_{ee} n_e / 2c \sim n_e / n(0) \quad , \quad (14)$$

where n(0) is the atomic oxygen density. At low altitudes electron-neutral particle collisions dominate electron-electron collisions and $b^2 << 4ac$. It follows that $\alpha_1 \simeq \alpha_2 = (c/a)^{1/2} \equiv \alpha >> 1/E_o$ and

$$\Phi(E) \simeq (4\pi)^{-1} \left(\frac{2}{m}\right)^{1/2} \frac{E}{(ac)^{1/2}} \left\{ \frac{S_o}{\alpha} \exp(-E/E_o) \right.$$

$$\left. + \frac{S_1}{2} \exp(-\alpha |E - E_1|) \right\} \quad . \quad (15)$$

The photoelectron flux again has a cust at E_1 and the line shape is symmetric with a half width given by $(a/c)^{1/2}$.

The second photoelectron source we examine is that due to a continuously decreasing source and the isolated photoionization source that is broadened.

$$S(E) = S_o \exp(-E/E_o) + S_1 \, r(E) \quad , \quad (16)$$

where r(E) is a rectangular function of height $1/2\Gamma$ and of width 2Γ centered about E_1. The photoelectron flux is given by Eq. (9) with f_1 replaced by f_1' where

$$f_1'(E) = \begin{cases} \dfrac{\sinh(\alpha_2\Gamma)}{\alpha_2\Gamma} \exp\left[\alpha_2(E-E_1)\right] & , \quad E<E_1-\Gamma \\ \dfrac{1-\exp\left[-\alpha_1(E-E_1+\Gamma)\right]}{2\alpha_1\Gamma} + \dfrac{1-\exp\left[\alpha_2(E-E_1-\Gamma)\right]}{2\alpha_2\Gamma} & , \quad E_1-\Gamma<E<E_1+\Gamma \\ \dfrac{\sinh(\alpha_1\Gamma)}{\alpha_1\Gamma} \exp\left[-\alpha_1(E-E_1)\right] & , \quad E_1+\Gamma<E \end{cases} . \tag{17}$$

Note that Φ has a rounded top and a continuous first derivative in the vicinity of E_1. Note also it is asymmetric at high altitudes ($\alpha_1>\alpha_2$) and symmetric at low altitudes ($\alpha_1\approx\alpha_2$). At altitudes above 260 km the forward half

$$\text{FHW} = T_e + \Gamma_e \left\{ \ln\left[\frac{\sinh(\Gamma/T_e)}{(\Gamma/T_e)}\right] - \ln\left[\frac{1}{2} + \frac{1-\exp(-\Gamma/T_e)}{2(\Gamma/T_e)}\right]\right\} \tag{18}$$

For simplicity we have neglected the shift in the location of the peak. For Γ comparable to T_e FHW is approximately $T_e+\Gamma - T_e \ln 2$. At low altitudes the half width is

$$\text{HW} = \left(\frac{a}{c}\right)^{1/2} + \left(\frac{a}{c}\right)^{1/2} \left\{ \ln\left[\sinh(\Gamma(c/a)^{1/2})\right] - \ln\left[1-\exp(-\Gamma(c/a)^{1/2})\right] \right\} . \tag{19}$$

For large $\Gamma(c/a)^{1/2}$ compared to 1, HW is approximately given by $(1-\ln 2)$ $(a/c)^{1/2} + \Gamma$.

2.2 RESULTS

Using the model ionosphere same as that given in Jasperse (1977), and using the Jacchia (1977) model for neutral atmosphere, we have calculated the theoretical photoelectron flux in the vicinity of the 27.2 eV peak at three altitudes. Results of these calculations are given in Jasperse and Smith (1978). The 27.2 eV peak was chosen as it is isolated and is produced only by photoionization

In comparing these calculations to the experimental results of Doering et al (1976), we see that the observed asymmetry and shift of the photoionization peak as the altitude increases is qualitatively explained by the BFP theory.

REFERENCES

Doering, J.P., W.K. Peterson, C.O. Bostrom, and T.A. Potemra, High resolution daytime photoelectron energy spectra from AE-E, Geophys. Res. Lett., 3, 129, 1976.

Jacchia, L.G., Thermospheric temperature, density, and composition: New models, Smithson. Astrophys. Observ. Spec. Rept., 375, 1977.

Jasperse, J.R., Electron distribution function in a nonuniform magnetized weakly photoionized gas application to a model ionosphere, AFCRL Rep. TR-75-0266, 1975.

Jasperse, J.R., Boltzmann-Fokker-Planck model for the electron distribution function in the Earth's ionosphere, Planet. Space Sci., 24, 33, 1976.

Jasperse, J.R., Electron distribution function and ion concentrations in the Earth's lower ionosphere from Boltzmann-Fokker-Planck theory, Planet. Space Sci., 25, 743, 1977.

Jasperse, J.R. and Ed R. Smith, Geophys. Res. Lett., 5, 843, 1978.

3 COLLISION OPERATOR STUDY

We have completed a systematic study of collisional operators based on the "velocity-ratio" expansion technique introduced originally by Schüller and Wilhelm[1]. This technique has been developed extensively by Ségur and Lerouvillois-Gaillard[2], and is applicable to all types of collisional processes involving light and heavy particles. It is particularly convenient when considering the impact of electrons with atoms, molecules, or ions. This calculational procedure considers systematically the dominant effects of the number density, temperature, drift, velocity-correlation tensor (or stress tensor) of the heavier species on the collisional operators of the transport equation for the distribution function of the lighter species.

In our study, we have considered the effects of ionization, dissociation, excitation, de-excitation, recombination, and Coulomb forces on the collisional operators. The following is a summary of the specific results of our investigation.

3.1 COLLISION OPERATORS VIA SCATTERING PROBABILITIES

In considering collisions between electrons and neutral species, we found it convenient to employ the "scattering probability" formulation of the Boltzmann-like operator. This idea was discussed by Waldmann[3] and used extensively by Desloge[4] and Ségur and Lerouvillois-Gaillard[2]. It allows us to treat all Boltzmann-like collision operators from a single unified viewpoint. We have used this procedure to consider the inelastic scattering between electrons and neutral species and electron-neutral impact ionization processes.

3.1.1 *Inelastic Scattering Between Electrons and Neutral Species*

We have considered the inelastic scattering of neutral particles (atoms and molecules) with colliding electrons. The atoms or molecules are allowed to undergo excitation and de-excitation processes. Principle of detailed balance is used to obtain the final form of the collision operator. The distribution functions of the neutral particles are assumed to be given but their functional forms can be quite arbitrary.

i) We have derived the collisional operator for excitation processes to second-order (in velocity-ratio) for an isotropic neutral distribution function. This result is the generalization of the classical expression developed by Holstein[5]. In the original expression of Holstein, the collision operator depends only on the number density of the colliding neutral species and the differential cross section. In our second-order calculation, the neutral temperature is also included in the final expression.

We have written the operator in an expanded form by writing the electron distribution function in spherical harmonics of the angles of the (electron) velocity vector. The first two moments of the operator have been obtained explicitly. They correspond to the isotropic part and the first anisotropic contribution of the collision operator. As a check, we have shown that in the limit of zero excitation energy, the isotropic part of the collision operator reduces to the classical Fokker-Planck form of the elastic collision operator.[6] Thus, the elastic collisional contribution is a second-order effect in terms of the ratio of the velocities of the colliding neutral particle and electron. It is not contained in the original Holstein expression.

ii) We have derived the corresponding collision operator to second order for de-excitation processes for an isotropic neutral distribution function. This is accomplished by applying the "principle of detailed balance" to the excitation and de-excitation processes. By expanding both the excitation and de-excitation operators in Taylor series in terms of the excitation energy and summing the resulting expressions, we obtain a generalized version of the Ginsburg-Gurevich-Allis[7] form of the isotropic part of the collision operator. In this calculation, we have assumed quasi-equilibrium of the neutral species and applied the Saha equation. Thus the effect of the neutral temperature is introduced in the collision operator through both the second-order velocity-correlation functions of the neutral species via the velocity-ratio expansion technique and also through the expansion of the Saha expression.

Our expression reduces to the classical Fokker-Planck form if only the terms to zeroth-order in velocity-ratio and second-order in excitation-energy are retained. [We note that this expression still contains the neutral temperature because of the Saha equation]. To second order in velocity-ratio, however, the structure of this collision operator is more complicated than the original Fokker-Planck form. We must be careful of not double-summing the elastic terms. Now the operator contains both first order and higher-order terms in excitation energy, as well as third and fourth order derivatives of the electron distribution function.

iii) We have derived the collision operator to first order (in velocity-ratio) for inelastic impact for an anisotropic neutral distribution function. This expression contains both the number-density and drift-velocity of the neutral species. We have expanded this operator in spherical harmonics of the angles of the (electron)

velocity vector. Since the spherical harmonics are no longer eigenfunctions of the collision operator, we find that the isotropic portion of the collision operator depends on the anisotropic part of the electron distribution function and vice versa.

3.1.2 Electron-Neutral Impact Ionization

We have considered the collision process of electrons and neutrals such that the neutrals are singly ionized by emitting secondary electrons. For simplicity, we have assumed that the neutral distribution function is isotropic. Thus, we shall neglect the effect of neutral drift on impact ionization.

The collision operator is found to depend on a double differential cross section as discussed, e.g., in Mott and Massey[8]. To second order (in velocity-ratio), our expression depends on the number density, and temperature of the neutral species. We have expanded the operator in spherical harmonics of the neutral species. We have expanded the operator in spherical harmonics of the (electron) velocity vector. The resulting expressions depend on the partial range integrals of the double differential cross section. Because of the impact and secondary electrons are indistinguishable after the collisional process, a factor of two (2) is introduced in some of the partial-range integrals.

To zeroth order (in velocity-ratio), the isotropic portion and the first anisotropic moment of this collision operator reduce to the expressions derived previously by Jasperse.[9]

3.1.3 Collision Operator for Dissociative Recombination

We are primarily interested in the recombinative processes of electrons with molecular ions such that the molecules are dissociated into two atoms (or molecules) upon collision. The inverse of such a process does not involve collisions with the electrons and this portion of the collision operator is independent of the electron distribution function. It is essentially a "source term". Thus, it will be convenient to consider the collision operator in two distinct parts: one involving the forward process which is a linear function of the electron distribution function and the other a source term.

To consider the part of the collision operator involving the forward recombinative process of electrons with molecular ions, we expand the differential cross section in terms of the "ion-electron velocity-ratio". The result

is a simple expansion of the collision operator for recombinative processes. The effects of the number density, drift, and temperature of the ion species come in naturally. To the zeroth order of this expansion, our result agrees with the classical expression. (See e.g., Jasperse[9].)

3.1.4 Effects of Ion Drift on the Fokker-Planck Operator for Electron-Ion Collisions

It is known that the Fokker-Planck form of the collision operator for charged particles can be deduced from the Boltzmann equation[10], Liouville Theorem or Markov processes[12]. In considering electron-ion collisions and the collision operator, it has been customary to assume a Maxwellian distribution for the ions. It is quite straightforward to generalize the expressions to arbitrary ion distributions using the velocity-ratio expansion technique. We have systematically derived the expanded operator to include the effects of the ion-drift and ion-stress-tensor. We have again splitted the resulting operator into an isotropic part and the first order anisotropic moment. Our results reduce to the classical expression in the limit of zero ion drift and isotropic ion distribution.

3.2 INTEGRATION OF THE ELECTRON TRANSPORT EQUATION IN APPLIED ELECTRIC AND MAGNETIC FIELDS

We have extended the previous calculations[9b] of the electron distribution function in the collisional region of the ionosphere to include the effects of the local electric and magnetic fields. In a local approximation, we shall assume that the E,B-fields are given. We found that the integration of the electron transport equation can be accomplished conveniently if we project the electron distribution function in three (3) special directions:

i) the direction of the electric field,

ii) the direction of the magnetic field, and

iii) a direction normal to both the electric and magnetic field.

We found that if, for the isotropic portion of the collision operator, we

i) neglect recombination and attachment,

ii) use the Ginsburg-Gurevich-Allis form of the inelastic collision operator, or expand the inelastic operator [to zero order of the velocity ratio] in Taylor series in terms of the excitation energy,

iii) linearize the electron-electron collision term,

iv) neglect the neutral and ion drifts,

v) approximate electron-neutral impact ionization as an excitation process and expand in Taylor series in terms of the excitation energy,

vi) consider photoionization, and the secondary electron production due to electron-neutral impact (estimated by the continuous slowing down approximation) as known sources, and use a combined collision frequency for the anisotropic part of the collision operator, the electron transport equation can be integrated in terms of simple quadratures. Interestingly, these quadratures can be integrated explicitly for simple but realistic variations of the cross sections as a function of the electron energy.

We note that the above integration is accomplished by simultaneously considering the isotropic and anisotropic portions of the transport equation for the electrons.

3.3 INTEGRATION OF THE ELECTRON TRANSPORT EQUATION IN THE ABSENCE OF AN ELECTRIC FIELD

In the absence of the elhctric field, we can integrate, in local approximation, the electron transport equation perturbatively. If we use the same type of approximations suggested in Section 2 for the collision operators, the isotropic part of the electron transport equation can be integrated explicitly. This expression is probably only valid in the electron energy range $\gtrsim 20$ eV, but should be quite accurate for the photoionization peaks regime and higher electron energy ranges.

The anisotropic part of the electron transport equation in terms of a single combined collision frequency can also be integrated in the presence of an applied magnetic field.

In an earlier study, Jasperse and Smith[9c] calculated the photoelectron flux in the vicinity of photoionization peaks in terms of a local Green's function solution for the isotropic part of the electron distribution function. We have applied the same idea to calculate the anisotropic effects in the presence of an applied magnetic field near photoionization peaks.

3.4 SUMMARY

We have completed a systematic study of the collision operators that appear in the electron transport equation using the velocity-ratio expansion technique.

Processes involving inelastic impact, excitation and de-excitation, ionization, dissociating, recombination and Coulomb collisions have been considered. We believe this research is the most comprehensive and systematic investigation of the collision operators for the scattering of light particles by heavy particles at the present time.

Upon making some plausible approximations we are able to integrate the electron transport equation in the presence of electric and magnetic fields in the local approximation.

We are in the process of preparing two separate manuscripts reporting these research findings.

REFERENCES

1. V. Schuller and J. Wilhelm, J. Beitr. Plasmaphys., 12, 349 (1972).
2. P. Ségur and J. Lerouvillois-Gaillard, J. Plasma Physics 16, 1 (1976).
3. L. Waldmann, Handbuch der Physik, Vol. 12 (Springer-Verlag 1958).
4. E. A. Desloge, Statistical Physics (Holt, Rinehart, and Winston 1966).
5. T. Holstein, Phys. Rev. 70, 367 (1946).
6. See e.g., I. P. Shkarofsky, T. W. Johnston, M. P. Bachynski, The Particle Kinetics of Plasmas (Addison-Wesley, 1966).
7. (a) V. L. Ginsburg and A. V. Gurevich, Usp. Fir. Nauk 70, 201 (Soviet Phys. Usp. 3, 115, 1960).
   (b) W. P. Allis, Handbook der Physik, Vol. 21 (Springer 1956).
8. N. F. Mott and H. S. W. Massey, Theory of Atomic Collisions (Oxford 1965).
9. (a) J. R. Jasperse, Planet. Space Sci., 24, 33 (1976).
   (b) J. R. Jasperse, Planet. Space Sci., 25, 743 (1977).
   (c) J. R. Jasperse and E. R. Smith, Geophys. Res. Lett., 5, 843 (1978).
10. M. Rosenbluth, W. M. MacDonald, D. L. Judd, Phys. Rev. 107, 1 (1957).
11. L. Landau, Physik Z. Sowjitumion, 10, 154 (1936).
12. S. Chandrasekher, Rev. Mod. Phys., 15, 31 (1943).

4 ELECTROSTATIC PLASMA INSTABILITIES OF E-REGION PHOTOELECTRON DISTRIBUTIONS

4.1 INTRODUCTION

An ionized region exists in the Earth's upper atmosphere, which extends from about sixty kilometers above the Earth's surface to several thousand kilometers and beyond. At low latitudes during day-light hours, this ionized region results primarily from the photoionization of the neutral atmospheric constituents by electromagnetic radiation from the sun. In the study of this ionized region there are many problems of interest which require a detailed knowledge of the electron energy distribution. Once the distribution function is known, various important physical quantities, such as the volume emission rates for the air glow radiation, electron heating rates, and electron temperature profiles, can be calculated.

Theoretically, the electron distribution function can be determined by invoking appropriate energy balance between the photoelectron production and the losses due to various inelastic processes. Several authors have investigated this problem. Most recently, Jasperse[1] has developed a complete kinetic theory, using the Boltzmann-Fokker-Planck method, in the sense that it determines the electron energy distribution and the ion concentrations in the lower ionosphere (E region) self-consistently, once the boundary conditions and the model ionosphere are specified. The low energy spectrum of the isotropic part of the distribution function is Maxwellian with temperatures a few hundredth of an eV. In the suprathermal part of the spectrum, most interesting feature occurs between 2 and 4 eV energy. In this energy range, the distribution function has a minimum at about 2.3 eV (Fig. 1). This is explained theoretically, since the cross section for the electron-impact excitation of vibrational states of N_2 has a maximum at 2.3 eV. Beyond 2.3 eV, the photoelectron flux rises sharply to a maximum at about 4 eV, as the excitation cross section decreases sharply. Beyond this energy the flux falls off as the cross section for the excitation of metastable states of atomic oxygen increases. The theoretical calculations (Fig. 1) show that this minimum in the spectrum is more and more pronounced at or below altitudes of 130 km. Above 130 km, the valley starts to be filled up, the peak-to-valley ratio decreases, until at or above 210 km the structure disappears completely. This disappearance can be attributed to the depletion of N_2 as well as to the gradual smoothing process arising from electron-electron collisions as the altitude increases.

Measurements of the electron energy distribution by Doering et al[2] and, most recently, by McMahon and Heroux[3], who studied specifically the 2-5 eV energy range with improved energy resolution of the apparatus, are in good agreement with the theoretical calculations of Jasperse[1] at and above 170 km. Below 170 km, the calculated values of the peak-to-valley ratios by Jasperse is somewhat larger than the observed values. The observations are in most striking disagreement with the theory below 130 km, where they show plateaus in the distribution functions in the 2-4 eV energy range.

This discrepancy between theory and observations suggests that in the low altitude regions (100~170 km) collisional processes alone cannot account for the observed photoelectron distributions. It is well-known that a homogeneous plasma in a magnetic field with isotropic distribution functions, can be unstable if a population of high energy particles is also present. This is precisely the situation in the lower ionosphere, and it is expected that the plasma instability will produce the anomalous diffusion in the velocity space through wave-particle interaction, which in turn will flatten the distribution functions in the 2-4 eV energy range. With this in mind, we consider here excitation of electrostatic instabilities in the ionospheric collisional plasma by the suprathermal electrons near the 4-eV maximum (Fig. 1). In particular, we consider the two most important instabilities, namely, the upper hybrid instability and the electron cyclotron instability; and discuss the linear growth rates and the wave spectra as functions of altitude. Bloomberg[4] has investigated the upper hybrid instability using the theoretical electron distribution function of Dalgarno et al[5]. His calculations show that the instability is inoperative at or below 160 km due to large collisional damping rate. Since Jasperse[1] gives more accurate[3] theoretical electron distribution functions and since we now have more accurate data for determining the relevant collision frequencies, it is worthwhile to reexamine the upper hybrid isntability.

In Sec. 4.2, we present the mathematical formulation leading to the dispersion relation. In Sec. 4.3, we solve the dispersion relation and determine the various growth rates, and the spectrum of the unstable waves.

4.2 MATHEMATICAL FORMULATION

Since we intend to study the instabilities driven by the suprathermal electrons near 4-eV maximum (Fig. 1), we assume that the equilibrium electron

population is composed of only two parts: a Maxwellian (thermal) population, and a suprathermal one with monotonically decreasing energy profile peaked at 4 eV. This is indicated by dotted lines in Figure 1. In doing so, we have ignored the high energy photoionization peaks in the tail of the actual electron distribution function. We further assume that the positive ions form a neutralizing background of constant density. This is justified since we consider waves with frequencies $\omega \gtrsim \omega_{pe}$, where ω_{pe} is the electron plasma frequency. Then the small amplitude perturbation of the electrons is governed by the following equations:

$$\frac{\partial f_j}{\partial t} + \underset{\sim}{v} \cdot \underset{\sim}{\nabla} f_j - \frac{e}{mc} (\underset{\sim}{v} \times \underset{\sim}{B}_o) \cdot \frac{\partial f_j}{\partial \underset{\sim}{v}} - \frac{e}{m} \underset{\sim}{E} \cdot \frac{\partial F_{oj}}{\partial \underset{\sim}{v}} = C(f_j) \tag{1}$$

$$\underset{\sim}{\nabla} \cdot \underset{\sim}{E} = -4\pi e \sum_j \int f_j \, d^3v \tag{2}$$

where $\underset{\sim}{B}_o$ is the earth's magnetic field, which is assumed to be uniform, $f_j(\underset{\sim}{r},\underset{\sim}{v},t)$ is the perturbed electron distribution function, $F_{oj}(v)$ is the equilibrium electron distribution function isotropic in velocity space, and $\underset{\sim}{E}$ is the electric field associated with the density perturbation. The index j labels the two kinds of electron population.

The collision term, $C(f_j)$, in Eq. (1) represents the electron-electron, electron-ion and the electron-neutral collisions. Explicit forms of these collision terms can be found in Ref. 6. In a weakly ionized gas such as the low altitude ionosphere of our interest, the frequencies of electron-electron and electron-ion collisions are small in comparison with the neutral and we need consider only the electron-neutral collisions. Furthermore, inelastic electron-neutral collisions are much less frequent than the elastic ones. However, the complexity of the exact elastic collision term makes the analysis intractable. To avoid this, we use a B-G-K type[7]

$$C(f_j) = -\nu_j f_j + \nu_j (n_j/n_{oj}) F_{oj}(v) \tag{3}$$

where

$$n_j = \int f_j d^3v$$

is the perturbed electron density, n_{oj} is the equilibrium density, and ν_j is the sum of the frequencies of elastic collisions between the j type electrons and the various neutral particles (N_2, O_2, O, etc.) present in the ionosphere.

This particular choice of the collision term, which conserves only the number of particles, is adequate to describe the electron-neutral collisions.

We notice that Eq. (1) can be written as

$$\frac{df_j}{dt} + \nu_j f_j = \frac{e}{m} E \cdot \frac{\partial F_{oj}}{\partial \underset{\sim}{v}} + \nu_j \left(\frac{n_i}{n_{oj}}\right) F_{oj} \tag{4}$$

where d/dt is the convective derivative taken along the unperturbed electron orbit in the magnetic field $\underset{\sim}{B}_o$. Integrating Eq. (4) with respect to t we obtain

$$f_j = \int_{-\infty}^{t} dt' \, e^{\nu_j(t'-t)} \left[\frac{e}{m} \underset{\sim}{E}(\vec{r}',t') \cdot \frac{\partial F_{oj}}{\partial \underset{\sim}{v}'} + \nu_j \frac{n_j(\vec{r}',t')}{n_{oj}} F_{oj}(v') \right] \tag{5}$$

where $\underset{\sim}{r}'(t')$ and $\underset{\sim}{v}'(t')$ are the unperturbed electron orbits. Since the collision frequency is much less than the cyclotron frequency, the electron orbits in lowest order are given by

$$x'-x = -\frac{v_\perp}{\Omega} \sin\phi + \frac{v_\perp}{\Omega} \sin(\phi-\Omega\tau)$$

$$y'-y = \frac{v_\perp}{\Omega} \cos\phi - \frac{v_\perp}{\Omega} \cos(\phi-\Omega\tau)$$

$$z'-z = -v_{\parallel}\tau$$

$$v_x' = v_\perp \cos(\phi-\Omega\tau)$$

$$v_y' = v_\perp \sin(\phi-\Omega\tau)$$

$$v_z' = v_{\parallel}$$

where $\tau = t-t'$, and we have chosen a cylindrical coordinate system in the velocity space with the z-axis along $\underset{\sim}{B}_o$, so that $\underset{\sim}{v} = (v_\perp\cos\phi, v_\perp\sin\phi, v_{\parallel})$. The orbits are taken to satisfy $\underset{\sim}{r}'(t'=t) = \underset{\sim}{r}, \underset{\sim}{v}'(t'=t) = \underset{\sim}{v}$, and $\Omega = eB_o/mc$ is the electron cyclotron frequency.

We use $\underset{\sim}{E} = -\underset{\sim}{\nabla}\Phi$, where Φ is the electrostatic potential, and choose perturbations of the form $f = \hat{f} \exp(i\underset{\sim}{k}\cdot\underset{\sim}{v} - i\omega t)$. Then

$$f_j(\underset{\sim}{k},\omega,\underset{\sim}{v}) \quad \int_0^\infty d\tau \left[-\frac{ie}{m}\hat{\Phi}\,\underset{\sim}{k}\cdot\left\{\hat{x}\cos(\phi-\Omega\tau)\,\frac{\partial F_{oj}}{\partial v_\perp} + \hat{y}\sin(\phi-\Omega\tau)\,\frac{\partial F_{oj}}{\partial v_\perp} + \hat{z}\,\frac{\partial F_{oj}}{\partial v_\parallel}\right\} + \frac{\nu_j}{n_{oj}}\hat{n}_n(\underset{\sim}{k},\omega)\,F_{oj}(v)\right] \exp i\underset{\sim}{k}\cdot(\underset{\sim}{r}'-\underset{\sim}{r}) + i(\omega+i\nu_j)\,\tau \qquad (6)$$

where we have used $F_{oj}(v') = F_{oj}(v)$. Integrating Eq. (6) over velocity space we can find $n_j(\underset{\sim}{k},\omega)$ in terms of $\hat{\Phi}(\underset{\sim}{k},\omega)$. Substituting for $\underset{\sim}{r}'-\underset{\sim}{r}$ and using azimuthal symmetry of the problem we can readily perform the ϕ-integration in velocity space and then the τ-integration.[8] The result can be expressed as

$$\hat{n}_j(\underset{\sim}{k},\omega) = \frac{N_j}{D_j}\,\hat{\Phi}(\underset{\sim}{k},\omega) \qquad (7)$$

where

$$N_j(k_\perp,k_\parallel,\omega) = \frac{2\pi e}{m}\sum_{n=-\infty}^{\infty}\int dv_\parallel dv_\perp v_\perp \frac{J_n^2(\frac{k_\perp v_\perp}{\Omega})}{\omega+i\nu_j - k_\parallel v_\parallel - n\Omega} \times\left(\frac{n\Omega}{v_\perp}\,\frac{\partial F_{oj}}{\partial v_\perp} + k_\parallel\frac{\partial F_{oj}}{\partial v_\parallel}\right) \qquad (8)$$

and

$$D_j(k_\perp,k_\parallel,\omega) \quad 1 - \frac{2\pi\nu_j i}{n_{oj}}\sum_{n=-\infty}^{\infty} dv_\parallel dv_\perp v_\perp \frac{J_n^2(\frac{k_\perp v_\perp}{\Omega})}{\omega+i\nu_j - k_\parallel v_\parallel - n\Omega} \qquad (9)$$

Substituting $\hat{n}_j$ into the Poisson equation (2), we obtain the dispersion relation

$$1 + \frac{4\pi e}{k^2}\sum_j (N_j/D_j) = 0 \quad , \qquad (10)$$

where $k^2 = k_\parallel^2 + K_\perp$.

4.3 STABILITY ANALYSIS

4.3.1 Resonant Type Instability

Here we look for instabilities that arise due to wave-particle resonant interactions. The waves are supported by the Maxwellian electrons, while they

are driven unstable by the suprathermal electrons near the 4 eV peak, which are in resonance with the waves. The resonance condition is $\omega_r - k_{\parallel} v_{\parallel} = n\Omega$, ω_r being the real part of the frequency. We first consider the properties of the waves by solving the dispersion relation without the suprathermal electron term, i.e., we solve the equation

$$1 + \frac{4\pi e}{k^2}\left(\frac{N_m}{D_m}\right) = 0 \tag{11}$$

where the subscript m refers to Maxwellian electrons. For Maxwellian electrons with density n_o and temperature T_e, the integrations in N and D can be carried out in a straightforward manner and the results are

$$N_m = \frac{en_o}{T_e}\left[1 + \frac{m}{2T_e}^{1/2}\frac{\omega + i\nu_m}{|k_{\parallel}|}\sum_{n=-\infty}^{\infty} Z(\rho_n)\, I_n(b)\, e^{-b}\right] \tag{12}$$

$$D_m = 1 + \left(\frac{m}{2T_e}\right)^{1/2}\frac{i\nu_m}{|k_{\parallel}|}\sum_{n=-\infty}^{\infty} Z(\rho_n)\, I_n(b)\, e^{-b} \tag{13}$$

Here $Z(\rho_n)$ is the plasma dispersion function, I_n is the modified Bessel function of first kind, $\rho_n = (\omega+i\nu_m-n\Omega)/[|k_{\parallel}|(2T_e/m)^{1/2}]$, $b = k_{\perp}^2 T_e/(\Omega^2 m)$. We shall consider waves for which $|\rho_n| >> 1$ for all n. This enables us to ignore the Landau damping. Using the asymptotic expansion for the Z function[9] and keeping the significant leading terms, we get

$$N_m \simeq -\frac{en_o}{m}\left[\frac{k_{\parallel}^2 I_o e^{-b}}{(\omega+i\nu_m)^2} + \frac{m}{T_e}\sum_{n=1}^{\infty}\frac{2n^2\Omega^2 I_n e^{-b}}{(\omega+i\nu_m)^2 - n^2\Omega^2}\right] \tag{14}$$

$$D_m \simeq 1 - \frac{i\nu_m}{\omega + i\nu_m}\left[1 + \sum_{n=1}^{\infty}\frac{2n^2\Omega^2 I_n e^{-b}}{(\omega+i\nu_m)^2 - n^2\Omega^2}\right] \tag{15}$$

We consider waves with $k_{\parallel}/k_{\perp} << 1$, and since $\nu_m << \omega, \omega_{pe}$, Eq. (11), with the aid of Eqs. (14) and (15),

$$1 - \frac{\omega_{pe}^2}{\omega(\omega+i\nu_m)}\left[\frac{k_{\parallel}^2}{k^2}e^{-b} I_o - \frac{k_{\perp}^2 e^{-b}}{k^2 b}\sum_{n=1}^{\infty}\frac{2n^2\omega_{pe}^2(\omega+i\nu_m) I_n}{\omega[(\omega+i\nu_m)^2 - n^2\Omega^2]}\right] = 0 \tag{16}$$

where $\omega_{pe} = (4\pi n_o e^2/m)^{1/2}$ is the electron plasma frequency. Expanding in $\nu_m/\omega << 1$ and keeping only the leading terms, we can write Eq. (16) in the form

$$\epsilon(k_\perp, k_\parallel, \omega) + i\frac{\nu_m}{\omega}\left[\frac{\omega_{pe}^2}{\omega^2}\frac{k_\parallel^2}{k^2} e^{-b} I_o + \frac{k_\perp^2 e^{-b}}{k^2 b} \sum_{n=1}^{\infty} \frac{2n^2\omega_{pe}^2(\omega^2+n^2\Omega^2) I_n}{(\omega^2-n^2\Omega^2)^2}\right] = 0 \tag{17}$$

where

$$\epsilon(k_\perp, k_\parallel, \omega) = 1 - \frac{\omega_{pe}^2}{\omega^2}\frac{k_\parallel^2}{k^2} e^{-b} I_o - \frac{k_\perp^2 e^{-b}}{k^2 b} \sum_{n=1}^{\infty} \frac{2n^2\omega_{pe}^2 I_n}{\omega^2 - n^2\Omega^2} \tag{18}$$

If we write $\omega = \omega_r + i\omega_i$, where $\omega_i << \omega_r$ in consistency with $\nu_m << \omega$, then ω_r is determined from

$$\epsilon(k_\perp, k_\parallel, \omega_r) = 0 \tag{19}$$

and ω_i is given by

$$\omega_i \simeq -\frac{(\nu_m/\omega_r)}{(\partial\epsilon/\partial\omega)_{\omega=\omega_r}}\left[1 + \frac{k_\perp^2 e^{-b}}{k^2 b} \sum_{m=1}^{\infty} \frac{4n^4\omega_{pe}^2 \Omega^2 I_n}{(\omega_r^2-n^2\Omega^2)^2}\right] \tag{20}$$

In deriving Eq. (20), which gives the collisional damping of the modes, we have made use of the dispersion relation (19).

The roots of the dispersion relation in the limiting case $k_\parallel=0$ was first discussed by Bernstein.[10] They depend on the values of the parameters: b and Ω^2/ω_{pe}^2. In the cold plasma limit $b<1$, and, furthermore, over the ionospheric region of our interest (100-170 km), $\Omega^2/\omega_{pe}^2 << 1$. Then, the lowest frequency

$$\omega_2 \simeq 2\Omega\left[1 - \frac{\omega_{pe}^2 b}{\omega_{pe}^2 - 3\Omega^2}\right], \quad \omega_{pe}^2 > 3\Omega^2 \tag{21}$$

The next higher frequency mode is the so-called upper hybrid mode:

$$\omega_{II} \simeq \left(\omega_{pe}^2 + \Omega^2\right)^{1/2} \tag{22}$$

The higher frequency modes (just above or just below the cyclotron harmonic depending on the value of ω_{pe}^2/Ω^2) are given by (n-3,4,....)

$$\omega_n \simeq n\Omega\ [1 - 0(b^{n-1})]\ ,\ \omega_{pe}^2 > (n^2-1)\ \Omega^2$$

$$\simeq n\Omega\ [1 + 0(b^{n-1})]\ ,\ \omega_{pe}^2 < (n^2-1)\ \Omega^2 \qquad (23)$$

These so-called Bernstein modes[10] are separated by frequency intervals where there is no propagation, i.e., $k_\perp^2 < 0$. In Eqs. (21) - (23) there are small corrections of the order of $k_\parallel^2/k_\perp^2 << 1$, which have been omitted for the sake of convenience. The corresponding damping rates are found to be

$$\omega_i \simeq 4\nu_m \frac{\Omega^2}{\omega_2^2}\left[1 - \frac{3}{8}\ \frac{\omega_{pe}^4\ b}{(\omega_{pe}^2-3\Omega^2)^2}\right]\ ; \qquad (24)$$

$$\simeq -\ \nu_m\left(\frac{\omega_H^2\ +\ \Omega^2}{2\omega_H^2}\right)\ ; \qquad (25)$$

$$\simeq -\ \nu_m\left(\frac{\omega_n^2\ +\ n^2\Omega^2}{2\omega_n^2}\right) \qquad (26)$$

respectively for the modes ω_2, ω_H, and ω_n.

In order to find the destablizing effect of the suprathermal electrons (denoted by a subscript h), we now consider the complete dispersion relation:

$$[\text{L.H.S. of Eq. (17)}] + (4\pi e/k^2)(N_h/D_h) = 0 \qquad (27)$$

where N_h and D_h are to be calculated from Eqs. (8) and (9) respectively. We write $\omega = \omega_r + i\omega_i + i\gamma$, where ω_i is the collisional damping rate given by Eq. (20), and γ is the growth rate. Since $\int F_{oh}\ d\underset{\sim}{v} = n_{oh} < n_o$, we can assume the the contribution of the suprathermal electrons to the dielectric response function and, hence, the growth rate is small. Then, as before, we obtain

$$\varepsilon(k_\perp, k_\parallel, \omega_r) = 0\ ,$$

which determines ω_r, and

$$\gamma = - \frac{4\pi e \left| \mathrm{Im}(N_h/D_h) \right|_{\omega=\omega_r}}{k^2 (\partial \varepsilon/\partial \omega)_{\omega=\omega_r}} \tag{28}$$

where $\varepsilon(k_\perp, k_\parallel, \omega)$ is the same as in Eq. (18). In doing so we have neglected the small contribution to ω_r from $\mathrm{Re}(N_h/D_h)$.

We first recognize that the collisions of the suprathermal electrons with the neutral species will somewhat detune their resonance with the waves. As a result, γ will be less than its collisionless value. However, the reduction is found to be negligibly small, e.g., $\gamma = \gamma_o[1 - 0(\nu_h/\Omega)]$, where $\nu_h/\Omega << 1$, γ_o being the collisionless growth rate. This can be easily verified by carrying out the calculation with a simple functional form for $F_{oh}(v)$, e.g., $F_{oh} = (n_{oh}/4\pi v_o^2)\, \delta(v - v_o)$, v_o being the speed corresponding to the peak energy. So, the dominant damping is that due to the collisions of the Maxwellian electrons and is given by Eqs. (24) - (26). For the sake of convenience, we shall omit ν_h from N_h and D_h. Then D_h becomes unity, and since F_{oh} is isotropic in velocity space N_h becomes

$$N_h = \frac{2\pi e}{m} \left[\omega \sum_{n=-\infty}^{\infty} \int dv_\perp \, dv_\parallel \frac{\partial F_{oh}}{\partial v_\perp} \frac{J_n^2(k_\perp v_\perp/\Omega)}{\omega - k_\parallel v_\parallel - n\Omega} - 2 \int_0^\infty dv \, v \frac{\partial F_{oh}}{\partial v} \right] \tag{29}$$

where $v^2 = v_\perp^2 + v_\parallel^2$. Substituting this into Eq. (28) and using the formula

$$\frac{1}{\omega - k_\parallel v_\parallel - n\Omega} = P \frac{1}{\omega - k_\parallel v_\parallel - n\Omega} - i\pi\delta(\omega - k_\parallel v_\parallel - n\Omega)$$

where the symbol P denotes the Cauchy principal value, we finally get

$$\gamma = \frac{2\pi^2 \omega_{pe}^2 \omega_r}{k_\perp^2 |k_\parallel| (\partial \varepsilon/\partial \omega)_{\omega=\omega_r}} \frac{n_{oh}/n_o}{} \sum_{n=-\infty}^{\infty} \int_0^\infty dv_\perp J_n^2 \left(\frac{k_\perp v_\perp}{\Omega}\right) \left(\frac{\partial \tilde{F}_{oh}}{\partial v_\perp}\right)_{v_\parallel = \frac{\omega_r - n\Omega}{k_\parallel}} \tag{30}$$

Here $\tilde{F}_{oh} = F_{oh}/n_{oh}$, so that $\int \tilde{F}_{oh} \, dv = 1$.

We change over to the energy representation using $G_{oh}(E) = (2^{1/2}E^{1/2}/m^{3/2})$ $F_{oh}(v)$, so that the normalization condition if $4\pi\int G_{oh}(E)\,dE = \int F_{oh}(v)\,d\underline{v} = 1$. Here $E = mv^2/2$ is the energy variable. In the energy representation, Eq. (30) becomes

$$\gamma = \frac{4\pi^2(n_{oh}/n_o)}{K_\perp^2|K_\parallel|(\partial\epsilon/\partial\omega)_{\omega=\omega_r}}\left(\frac{\omega_{pe}^2\omega_r}{\Omega^3}\right)E_o^{3/2}\sum_{n=-\infty}^{\infty}\int_{E_n}^{\infty}dE\,\frac{d}{dE}\left(\frac{G_{oh}}{E^{1/2}}\right)J_r^2\left(K_\perp\left(\frac{E-E_n}{E_o}\right)^{1/2}\right) \tag{31}$$

where $E_o = mv_0^2/2$ is the peak energy of the suprathermal electrons, $K_\parallel = k_\parallel v_o/\Omega$, $K_\perp = k_\perp v_o/\Omega$, and $E_n = E_o[(\omega_r/\Omega - n)/K_\parallel]^2$. Integrating by parts and using a Bessel function identity we rewrite Eq. (31) in the more convenient form

$$\gamma = \frac{\pi^2(n_{oh}/n_o)}{|K_\parallel|(\partial\epsilon/\partial\omega)_{\omega=\omega_r}}\left(\frac{\omega_{pe}^2\omega_r}{\Omega^3}\right)\sum_{n=-\infty}^{\infty}\frac{E_o^{1/2}}{n}\int_{E_n}^{\infty}\frac{dE}{E^{1/2}}\,G_{oh}(E)\,|J_{n+1}^2 - J_{n-1}^2| \tag{32}$$

The behavior of the functions in the integrand of Eq. (32) is shown in Figure 2. It is clear that to obtain large contribution to the integral we must choose a value of E_n smaller than E_o. This sets a lower limit to $K_\parallel$. For a given ω_{pe}/Ω, which depends on the altitude, ω_r may be such that $\omega_r/\Omega - n$ is smallest for n=p (say). The corresponding lower limit for $K_\parallel$ is fixed by requiring that $E_p < E_o$. Next, we note that $J_{p+1}^2 - J_{p-1}^2$ is an oscillating function of the argument with progressively decreasing amplitude. Since the maximum contribution of G_{oh} comes from the vicinity of $E=E_o$ and since G_{oh} is strongly peaked at $E=E_o$, a positive value of the integral (meaning instability) will be obtained whenever $K_\perp(1-E_p/E_o)^{1/2}$ falls within the positive domain of $J_{p+1}^2 - J_{p-1}^2$. In other words, the regions of unstable $K_\perp$ will alternate with those of stable $K_\perp$. The largest positive value of the integral will, of course, be obtained when $K_\perp(1-E_p/E_o)^{1/2}$ is equal to the value at which the first maximum of $J_{p+1}^2 - J_{p-1}^2$ occurs. However, for the same values of ω_{pe}/Ω and $K_\perp$, which ensure the positiveness of the n=p term, there will be some or all $n\neq p$ for which the value of $K_\perp(1-E_n/E_o)$ may be such that $J_{n+1}^2 - J_{n-1}^2$ is negative. These terms in the sum may cancel the positive contribution from the n=p term and thus eliminate the instability. However, if we choose $K_\parallel$ in such a way that $E_p < E_o$, but $E_n > E_o$ for all $n\neq p$, then the negative contribution from the $n\neq p$ terms will be comparatively small and the dominant contribution to γ will arise from the n=p term in the sum. This sets an upper limit to $K_\parallel$. The optimal value of $K_\parallel$ is determined by the width of $G_{oh}(E)$. Finally, we observe that the upper hybrid mode has the largest growth rate in comparison with the Bernstein (cyclotron harmonic) modes.

This is so because $\partial\omega/\partial\omega$ is large near the cyclotron harmonics ($\sim b^{1-n}$, n=2,3,4, ...). Hence, we shall concentrate on the upper hybrid instability. In this case,

$$\omega_r = \omega_H = \Omega\left(1+\omega_{pe}^2/\Omega^2\right)^{1/2} , \qquad (22')$$

and

$$\gamma = \frac{\pi^2}{2}\left(\frac{n_{oh}}{n_o}\right)\Omega\left(\frac{\omega_{pe}}{\Omega}\right)^4 \frac{E_o^{1/2}}{|K_{\parallel}|}\sum_{n=-\infty}^{+\infty}\frac{1}{n}\int_E^{\infty}\frac{dE}{E^{1/2}}G_{oh}(E)\,(J_{n+1}^2 - J_{n-1}^2) , \qquad (32')$$

where the arguments of J_{n+1}^2 and J_{n-1}^2 are the same as that of J_n^2 in Eq. (31).

In order to obtain values of γ we now consider the parameters of our interest. In the lower ionosphere (100~170 km), $n_o = (0.6\sim3.0)\times10^5\ cm^{-3}$, $B_o \simeq 0.35G$; then, $\omega_{pe}/\Omega \simeq 2.24$ 5.0. Numerical values of γ have been obtained using the electron energy distributions of Jasperse[1]. The collision frequencies, ν_m, have been calculated using the recent cross section data, and the model atmosphere of Jacchia[11]. Electron temperatures were taken from Jasperse[1] calculations. The collisional damping rates are given by Eq. (25). Results of these calculations are summarized in Table 1. The maximum value of the growth rate, γ_m, corresponds to the maximum value of the sum appearing in Eq. (32'). We notice that γ_m increases with altitude. This is mainly due to the fact that both ω_{pe}/Ω and n_{oh}/n_o increase with altitude [see Eq. (32')]. The integral in Eq. (32') decreases with altitude due to broadening of the distribution function, but the decrement is very small over the altitude regions of our interest. We have verified it further by evaluating the integrals with $G_{oh} = \delta(E-E_o)/4\pi$ and then comparing these with the actual numerical values. The collision frequency and, hence, the damping rate ω_i decreases with altitude. This is due to tion of neutral species. At higher altitudes, however, electron-electron and electron-ion collisions, not considered in this work, become increasingly important.

We further notice that the value of $k_\perp v_o/\Omega$ for which the growth rate is maximum increases with altitude. So, b $k_\perp^2 T_e/m\Omega^2 = (k_\perp^2 v_o^2/\Omega^2)T_e/2E_o$) increases with altitude and becomes finite. Consequently, the growth rates in Table 1, which are obtained for $b\ll1$, have to be modified. From the dispersion relation (19) we find that the finite-b-modified upper hybrid mode has a frequency larger than its previous value. For example, when $\omega_{pe}/\Omega = 4.3$ (140 km) $b\simeq1.0$ and then the frequency is $\omega_{II}\simeq5.4\Omega$ whereas, for $b\ll1$, $\omega_{II}\simeq4.14\Omega$ (see Ref. 10 for

the solutions of the dispersion relation when b is finite). This means that instead of n=4, n=5 term will contribute most to the integral in Eq. (32'). The growth rate will be smaller than the one reported in Table 1, but the reduction is small. At high altitudes electron-electron collisions, not considered in this work, will be more effective in eliminating the instability.

Finally, at altitudes below 125 km the collisional damping rate exceeds the maximum growth rate of the upper hybrid mode, and so the instability cannot be excited. As we show in the next section, below 125 km a different type of instability, namely, the electrostatic electron cyclotron instability, can be excited.

4.3.2 Electron Cyclotron Instability

In the previous section we considered unstable waves with small but finite $k_{\parallel}$. Here we show that under certain conditions waves propagating strictly across the magnetic field ($k_{\parallel}=0$) can also be driven unstable by the suprathermal electrons. This instability, which is of non-resonant type, is excited at the electron cyclotron harmonics. In order to calculate N_h and D_h for this case, we change over to the spherical coordinates in the velocity space and after some straightforward algebra (see Appendix) obtain

$$N_h = \frac{4\pi e}{m} \int_0^\infty dv\, F_{oh}(v) \left[1 - (\omega+i\nu_h) \sum_{n=-\infty}^{\infty} \frac{J_{2n}(2k_\perp v/\Omega)}{\omega+i\nu_h - n\Omega}\right] \tag{33}$$

$$D_h = 1 - \frac{4\pi\Omega}{k_\perp^2 n_{oh}} \sum_{n=-\infty}^{+\infty} \frac{i\nu_h}{\omega+i\nu_h-n\Omega} \int_0^\infty dv\, v\, F_{oh}(v) \sum_{p=0}^{\infty} J_{2n+2p+1}(2k_\perp v/\Omega) \tag{34}$$

In deriving Eqs. (33) and (34) we have put $k_\parallel=0$. The complete dispersion relation is then

$$1 - \sum_{n=1}^{\infty} \frac{2n^2\omega_{pe}^2(\omega+i\nu_m)\, a_n}{\omega[(\omega+i\nu_m)^2 - n^2\Omega^2]} + \frac{4\pi e}{k_\perp^2}\left(\frac{N_h}{D_h}\right) = 0 \tag{35}$$

where N_h and D_h are given by Eqs. (33) and (34), $a_n = (I_n/b)\exp(-b)$ [see Eq. (16)], and we have denoted k by $k_\perp$. Let us first analyze the dispersion relation in the limit $\nu_m=0$. We write $\omega=n\Omega(1+\chi)$, where $n\geq 2$ and $\chi \ll 1$ (since $n_{oh}/n_o \ll 1$). Then, Eq. (35) becomes

$$1 - \frac{2a_1\omega_{pe}^2}{(n^2-1)\Omega^2} + \frac{4a_1\chi n^2\omega_{pe}^2}{(n^2-1)^2\Omega^2} - \frac{\omega_{pe}^2}{\chi\Omega^2}\left(a_n + \frac{\sigma I\Omega^2}{k_\perp^2 v_o^2}\right) = 0 \tag{36}$$

Here $\sigma = n_{oh}/n_o$ and the quantity I is defined as

$$I(n) = 4\pi v_o^2 \int_o^\infty dv\, F_{oh}(v)\, J_{2n}(2k_\perp v/\Omega) \quad , \quad n \geq 2 \quad , \tag{37}$$

where $F_{oh} = F_{oh}/n_{oh}$, and $mv_o^2/2 = E_o$ is the peak energy of the suprathermal electrons. We have neglected terms of the order of $(\nu_h/n\Omega)\sigma$ or smaller compared to the others. One of the roots of the algebraic equation (36) is

$$\chi = \frac{n^2-1}{4n^2}\left[1 - \frac{(n^2-1)\Omega^2}{2a_1\omega_{pe}^2}\right]$$

$$+ \left\{\frac{(n^2-1)^2\Omega^4}{64a_1^2n^4\omega_{pe}^4}\left[1 - \frac{2a_1\omega_{pe}^2}{(n^2-1)\Omega^2}\right]^2 + \frac{(n^2-1)^2}{4a_1n^2}\left(a_n + \frac{\sigma I\Omega^2}{k_\perp^2 v_o^2}\right)\right\}^{1/2} \tag{38}$$

We notice from Eq. (38) that χ can have a positive imaginary part (meaning instability) when $I<0$,

$$|I| > \frac{a_n k_\perp^2 v_o^2}{\sigma\Omega^2} \tag{39}$$

and,

$$\left|1 - \frac{2a_1\omega_{pe}^2}{(n^2-1)\Omega^2}\right| < \frac{4na_1\omega_{pe}^2}{(n^2-1)\Omega^2}\left(\frac{\sigma|I|\Omega^2}{k_\perp^2 v_o^2} - a_n\right)^{1/2} \tag{40}$$

The condition (40) determines the range of the values of ω_{pe}^2/Ω^2 in which the n-th cyclotron harmonic can be unstable. The largest value of $\mathrm{Im}\chi$ is obtained when

$$\frac{\omega_{pe}^2}{\Omega^2} = \frac{n^2-1}{2a_1} \tag{41}$$

Then, χ becomes

$$\chi = i \frac{(n^2-1)\Omega}{nk_\perp v_o} \left[\frac{\sigma}{4a_1}\left(|I| - \frac{a_n k_\perp^2 v_o^2}{\sigma\Omega^2}\right)\right]^{1/2} \tag{42}$$

The second term within the parenthesis in Eq. (42) represents the finite-b stabilizing effect. In the presence of collisions, the solution of the complete dispersion relation (35) is

$$\omega = n\Omega + i\left[\gamma - \frac{(n^2+1)\nu_m}{4n^2}\right], \quad n \geq 2 \tag{43}$$

where $\gamma = n\Omega(Im\chi)$ and the additional term is the collisional damping rate. The maximum value of the collisionless growth rate, denoted by γ_m, is

$$\gamma_m \simeq \frac{(n^2-1)\Omega}{k_m}\left[\frac{\sigma}{4a_1}\left(\max|I| - \frac{a_n k_m^2}{\sigma}\right)\right]^{1/2} \tag{44}$$

Here k_m is the value of $k_\perp v_o/\Omega$ for which the maximum value of $|I|$ is obtained. Finally, the condition for exciting the electron cyclotron instability in the presence of electron-neutral collisions is

$$\gamma_m > \frac{(n^2+1)\nu_m}{4n^2} \tag{45}$$

Although accurate determination of I requires numerical integration, it is possible to obtain an analytic expression for I using a suitable F_{oh} that closely represents the actual distribution function. Such an analysis is instructive, if not so accurate. We first change over to the energy representation so that Eq. (37) becomes

$$I = 4\pi E_o \int_o^\infty \frac{dE}{E} G_{oh}(E) J_{2n}\left[\frac{2k_\perp v_o}{\Omega}\left(\frac{E}{E_o}\right)\right]^{1/2} . \tag{46}$$

We then choose

$$G_{oh}(E) = \frac{\alpha^{1+\alpha}}{4\pi E_o \Gamma(1+\alpha)}\left(\frac{E}{E_o}\right) \exp(-\alpha E/E_o) , \tag{47}$$

which satisfies the required normalisation condition: $4\pi\int_0^\infty G_{oh}(E) = 1$. It can be easily verified that such a distribution is peaked at $E=E_o$, and the quantity α is a measure of the width of the distribution, e.g., $\alpha=4(E_o/\Delta)^2$, where Δ is the characteristic half-width of the distribution. Our model distribution closely resembles the ones that are found in the low altitude regions by theoretical calculation.[1] Substituting this $G_{oh}(E)$ into Eq. (46) we find[12]

$$I = \frac{(k_\perp v_o/\Omega)^{2n}\Gamma(n+\alpha)}{\alpha^{n-1}\Gamma(1+\alpha)\Gamma(2n+1)} \exp(-k_\perp^2 v_o^2/\alpha\Omega^2)\, M(n+1-\alpha;2n+1;k_\perp^2 v_o^2/\alpha\Omega^2) \qquad (48)$$

where M is the confluent hypergeometric function. From the properties of the function M we find that I will be negative when $(n+1\alpha) < 0$, provided $(k_\perp^2 v_o^2/\alpha\Omega^2) > 1$. This condition tells us that for the n-th cyclotron harmonic to be unstable the width of the electron distribution has to be such that $(\Delta/2E_o) < (n+1)^{-1/2}$, i.e., for large n, the distribution function has to be very narrow; otherwise, the mode will be stable. We have shown earlier [Eq. (41)] that the value of unstable n is determined by the value of ω_{pe}/Ω. Since ω_{pe}/Ω increases with altitude, requiring larger n values for the instability to set in, and since the widths of the calculated distribution functions also increase with altitude (see Fig. 1), we can conclude that the cyclotron instability will be operative only in the low altitude regions. The approximate width of the unstable spectrum is given by

$$\pi^2 (n+\tfrac{3}{4})^2/(4\alpha-2) < \frac{k_\perp^2 v_o^2}{\alpha\Omega^2} < \pi^2 (n+\tfrac{7}{4})^2/(4\alpha-2) \qquad (49)$$

since M is negative within this region. There are, of course, other regions of negative M corresponding to higher values of $k_\perp v_o/\Omega$, but for those values I will be smaller in magnitude. We can obtain the approximate value of I by taking the $\alpha \to 1$ limit, in which case $G_{oh} \to \delta(E-E_o)/4\pi$, and Eq. (48) reduces to

$$I = J_{2n}(2k_\perp v_o/\Omega) \qquad (50)$$

Numerical calculations using the theoretical distributions of Jasperse[1] indicate that Eq. (50) is an excellent estimate for I in the low altitude regions of our interest. For illustration purpose, let us consider the n=4 mode. If we take $B_o = 0.35G$, the value of ω_{pe}/Ω given by Eq. (41) [with $2a_1=1$] then

corresponds to the electron density at an altitude ~130 km. From Eq. (50), $\max|I| = \max(-J_8) \approx 0.23$, corresponding to $k_\perp v_o/\Omega = 7.1$. Numerical evaluation of Eq. (46) for n=4, using actual $G_{oh}(E)$, yields $\max|I| \approx 0.18$, which is obtained for $k_\perp v_o/\Omega = 7.1$. The agreement is even better at lower altitudes where $G_{oh}(E)$ is narrower.

In so far as the stabilizing term in Eq. (44) due to finite-b effect can be neglected, the collisionless growth rate of the electron cyclotron instability is large compared to that of the upper hybrid instability. In the former case, growth rate is proportional to $\sigma^{1/2}$ while in the latter case it is proportional to σ, where $\sigma = n_{oh}/n_o \ll 1$. In Table 2 we present maximum collisionless growth rate (without the finite-b effect), and collisional damping rate as functions of altitude. The altitude is determined from the value of ω_{pe}/Ω, which in turn is determined by the cyclotron harmonic n according to Eq. (41).

As the altitude increases, the finite-b stabilizing effect becomes increasingly important. This is due to the fact the electron temperature as well as k_m increase with altitude. For n=4 mode, if we take into account the finite-b effect the reduced growth rate $\tilde{\gamma}_m$ is found to be $\gamma_m \approx 10^4 s^{-1}$. Above this altitude, the stabilizing term dominates and so the modes are stable.

4.4 SUMMARY AND DISCUSSION

We have studied the electrostatic instabilities associated with the E region (below 170 km) photoelectron distribution functions in the presence of electron-neutral collisions. We find that at low altitude (at or below 130 km) waves at electron cyclotron harmonics can become unstable with growth rates larger than the collisional damping rates. As altitude increases, this electron cyclotron instability is extinguished by finite-b ($k_\perp^2 T_e/m\Omega^2$) effect.

At altitudes 130 km and above, on the other hand, upper hybrid instability can be excited effectively. Our calculations based on the recent theoretical electron energy profiles of Jasperse[1] show that the upper hybrid instability can operate at altitudes as low as 120 km. This is an improvement over the calculation of Bloomberg[4], who found that the upper hybrid mode is stabilized by collisions at or below 160 km. This disagreement with Bloomberg's calculation is primarily due to the fact that he considered the collision frequencies of the 4 eV electrons. But, as we have shown in the text, the damping is mainly due to the Maxwellian electrons with temperature 0.04 eV at 120 km. Consequently, the relevant collision frequency is an order of magnitude

smaller than that of Bloomberg. Also, our calculated collisionless growth rates are somewhat larger than those due to Bloomberg. This can be attributed to our use of the electron energy distribution of Jasperse[1], which we believe is more accurate. At high altitudes (above 170 km) electron-electron collisions, not taken into account in this work, are expected to eliminate the upper hybrid instability.

Both of these instabilities are driven by the suprathermal electrons with energy peaked at 4 eV. Turbulence arising from these instabilities is expected to produce the observed[2,3] anomalous structure in the electron distribution function in the 2-4 eV energy range. This will be the topic of our future work.

REFERENCES

1. J. R. Jasperse, Planet. Space Sci., 25, 743 (1977). For previous works, see the references cited herein.

2. P. J. Doering, W. G. Fastie, and P. D. Feldman, J. Geophys. Res., 75, 1787 (1970).

3. W. J. McMahon and L. Heroux, Air Force Geophysics Laboratory Report AFGL-TR-77-0013 (Bedford, Massachusetts, 1977).

4. H. W. Bloomberg, J. Geophys. Res., 80, 2851 (1975).

5. A. Dalgarno, M. B. McElroy, and A. I. Stewart, J. Atmos. Sci., 26, 753 (1969).

6. I. P. Shkarofsky, T. W. Johnston, and M. P. Bachynski, The Particle Kinetics of Plasmas, Addison-Wesley Publishing Company, Reading, Massachusett (1966).

7. P. L. Bhatnagar, E. P. Gross, and M. Krook, Phys. Rev., 94, 511 (1954).

8. S. Ichimaru, Basic Principles of Plasma Physics, W. A. Benjamin, Inc., Reading, Massachusetts (1973), p. 50.

9. B. D. Fried and S. D. Conte, The Plasma Dispersion Function, Academic Press, New York (1961).

10. I. B. Bernstein, Phys. Rev. 109, 10 (1958).

11. L. G. Jacchia, Smithson. Astrophys. Observ. Spec. Rept. 375, Cambridge, Massachusetts (1977).

12. I. S. Gradshteyn and I. M. Ryzhik, Tables of Integrals, Series, and Products, Academic Press, New York (1965), p. 716.

5 APPROXIMATE ANALYTIC SOLUTIONS FOR THE AURORAL PROTON AND HYDROGEN FLUXES AND RELATED QUANTITIES

5.1 INTRODUCTION

The proton aurora results from the precipitation of energetic (~1 to 100 keV) protons, with the peak of the energy spectrum lying below 10 keV, into the auroral atmosphere. Spectroscopically, it is identified by the readily detectable Balmer series emissions (H_α, H_β, and H_γ). The Balmer emissions are radiated by the moving hydrogen atoms that are produced in the charge-exchange collisions of the protons with the atmospheric constituents. The proton precipitation also results in the excitation of various nitrogen and oxygen emissions, such as λ3914, λ4709 N_2^+, and λ5577 OI.

Theoretical calculations of energy deposition function, ionization rate, and λ3914 N_2^+/H_β intensity ratio were initiated by Chamberlain [1961]. Since then, Eather and his co-workers have improved upon Chamberlain's calculations utilizing recent experimental and theoretical cross sections for all the energy loss processes involved. A complete list of these works can be found in the monograph by Vallance Jones [1974]. These calculations, however, are semi-empirical in nature, without the detailed knowledge of the energy distribution and the pitch angle distribution of the precipitating protons as a function of altitude. As Eather [1967] has pointed out both the energy spectrum and the pitch angle distribution must be known for correct theoretical interpretation of the measured hydrogen line profiles.

In this paper, we calculate for the first time the energy and pitch angle distribution of the auroral protons as a function of altitude, applying the methods of linear transport theory. The proton precipitation problem is complicated by the partial neutralization of the incident protons as a result of the charge-exchange collisions. This leads to a coupled set of transport equations - one for the proton flux, and the other for the neutral hydrogen atom flux. Another related complication is that the hydrogen atom resulting from the charge-exchange collision can travel large distances across the earth's magnetic field lines before being converted back to a proton via charge-stripping reaction. Davidson [1965] used a Monte Carlo technique to analyze this transverse diffusion and found that, for 5 to 20 keV protons, for example, an isotropic incident pitch angle distribution results in a spreading of the

precipitation zone over an area as wide as 600 km. Consequently, the relevant transport problem is, strictly speaking, a two-dimensional one. In the present work, we ignore this transverse diffusion and obtain approximate analytic solutions for the proton and the hydrogen fluxes in a plane-parallel geometry. We also present analytic expressions for energy deposition rate, and ionization rate as a function of altitude. In Sec. , we calculate these quantities as well as the density of electrons, which result from ionization and the stripping of H atoms, for an isotropic-Maxwellian incident proton flux, using the pseudoparticle method of Jasperse and Strickland [1979].

5.2 CHARACTERISTIC FEATURES OF PRECIPITATING PROTONS

Fast protons entering the upper atmosphere undergo charge-exchange collisions in which the incident proton captures an electron and becomes a fast hydrogen atom. The H atom then undergoes stripping producing a proton and an electron, thus completing the charge-changing cycle. These processes are:

$$H^+ + M \rightarrow H + M^+ \tag{1}$$

$$H + M \rightarrow H^+ + M + e^- \tag{2}$$

where M denotes any atmospheric constituent. The cross sections for these processes are quite large ($\geq 10^{-16}$ cm^2). As a consequence, an initially pure H^+ flux soon becomes a mixture of H^+ and H, and after only a few charge-changing cycles an equilibrium flux is established in which the fractional composition is a function of energy. For auroral energies, this equilibriation occurs well above the altitude where significant energy losses due to ionization and excitation of the atmospheric constituents can occur.

In addition to processes (1) and (2), charge-changing processes such as

$$H^+ + M \rightarrow H^- + M^{++} \tag{3}$$

$$H^- + M \rightarrow H^+ + M + 2e^- \tag{4}$$

can occur. However, the cross sections for these processes are very small and the H^- content of the equilibrium flux is $\leq 1\%$ in the auroral energy range. Because ionization and excitation processes involving H^- have cross sections

comparable to those of H^+ and H processes, it is a good approximation to neglect H^- in the proton auroral analysis.

5.3 BASIC EQUATIONS

For a single constituent atmosphere, the linear transport equations for energetic protons and hydrogen atoms in a plane-parallel geometry are

$$\left[\mu\frac{\partial}{\partial z} + n(z)\left\{\sigma_p^i(E) + \sigma_p^{ex}(E) + \sigma_p^{e\ell}(E) + \sigma^{10}(E)\right\}\right]\Phi_p(z,E,\mu)$$

$$= 2\pi n(z) \sum_j \int dE'd\mu' \sum_k \sigma_{pj}^k(E',\mu' \to E,\mu)\ \Phi_p(z,E',\mu')$$

$$+ 2\pi n(z) \sum_j \int dE'd\mu'\ \sigma_j^{01}(E',\mu' \to E,\mu)\ \Phi_H(z,E',\mu') \qquad (5)$$

$$\left[\mu\frac{\partial}{\partial z} + n(z)\left\{\sigma_H^i(E) + \sigma_H^{ex}(E) + \sigma_H^{e\ell}(E) + \sigma^{01}(E)\right\}\right]\Phi_H(z,E,\mu)$$

$$= 2\pi n(z) \sum_j \int dE'd\mu' \sum_k \sigma_{Hj}^k(E',\mu' \to E,\mu)\ \Phi_H(z,E',\mu')$$

$$+ 2\rho n(z) \sum_j \int dE'd\mu'\ \sigma_j^{10}(E',\mu' \to E,\mu)\ \Phi_p(z,E',\mu') \qquad (6)$$

where Φ's are the particle fluxes, z is the altitude, μ is cosine of the angle between the particle velocity and the positive z-axis, which is parallel to the geomagnetic field lines, and $n(z)$ is the neutral density. Here, $\sigma_j^k(E',\mu' \to E,\mu)$ is the differential cross section per unit range (referred to hereafter as just the differential cross section) for collision between the precipitating particles and the neutral particles in which the neutral particle makes a transition from the ground state to the final state j. The summation index k labels elastic ($e\ell$), excitation (ex), and ionization (i)-type collisions. The corresponding total cross sections, denoted by $\sigma^k(E)$, is related to the differential cross sections by the formula

$$\sigma^k(E) = 2\pi \sum_j \int dE'd\mu'\ \sigma_j^k(E',\mu' \to E,\mu) \qquad (7)$$

The subscripts P and H represent cross sections associated with the protons and the hydrogen atoms respectively. In addition, σ_j^{10} is the differential cross section for the charge-exchange process (1) in which the ionized neutral particle is left in the state j, and σ_j^{01} is the equivalent differential cross section for the stripping process (2). The corresponding total cross sections, $\sigma^{10}(E)$ and $\sigma^{01}(E)$, are related to the differential cross sections by the formulae similar to Eq. (7).

In writing Eqs. (5) and (6) we have ignored any electric field that may be present in the auroral atmosphere and assumed that the geomagnetic field is uniform. Under these assumptions, protons lose energy only via collisions and such collisions result in discrete energy losses.

5.4 FORWARD-SCATTERING AND AVERAGE DISCRETE ENERGY-LOSS APPROXIMATIONS

The differential cross sections for all the processes involving protons and H atoms are very strongly peaked in the forward direction for incident energies above a few hundred eV [McNeal and Birely, 1973]. This suggests that except toward the end of the precipitation one can make the forward scattering approximation. We shall use this simplifying approximation with the understanding that our analysis will be only valid for $E>E_{min}$.

The loss function L(E), the energy loss per unit path length per molecule, for a particular inelastic process (excitation, ionization, charge-exchange or stripping) may simply be defined as the product of the average energy loss W and the total cross section associated with the process. Edgar et al [1973] have given the loss function for each inelastic process as a function for each inelastic process as a function of proton energy. Using the cross sections given by McNeal and Birely [1973], and assuming equal average energy loss for both protons and H atoms, we have calculated W as a function of E from the loss functions of Edgar et al [1973] and find that it is a weak function of energy in the auroral energy range and that it is almost the same for all the inelastic processes. In the average discrete energy-loss approximation, W is taken to be a constant (= 28 eV) and the same for all the inelastic processes.

With these approximations, we write

$$\sigma^{e\ell}(E',\mu' \cdot E,\mu) = (2\pi)^{-1} \sigma^{e\ell}(E') \delta(E'-E) \delta(\mu'-\mu) \qquad (8)$$

$$\sum_j \sigma_j^{ex}(E',\mu' \to E,\mu) = (2\pi)^{-1} \sum_j \sigma_j^{ex}(E') \, \delta[E'-(E+W)] \, \delta(\mu'-\mu) \tag{9}$$

$$\sum_j \sigma_j^{i}(E',\mu' \to E,\mu) = (2\pi)^{-1} \sum_j \sigma_j^{i}(E') \, \delta[E'-(E+W)] \, \delta(\mu'-\mu) \tag{10}$$

$$\sum_j \sigma_j^{10}(E',\mu' \to E,\mu) = (2\pi)^{-1} \sum_j \sigma_j^{10}(E') \, \delta[E'-(E+W)] \, \delta(\mu'-\mu) \tag{11}$$

$$\sum_j \sigma_j^{01}(E',\mu' \to E,\mu) = (2\pi)^{-1} \sum_j \sigma_j^{01}(E') \, \delta[E'-(E+W)] \, \delta(\mu'-\mu) \tag{12}$$

for both protons and H atoms. Here, $\sum_j \sigma_j^{ex}(E')$ is the total excitation cross section $\sigma^{ex}(E')$, and so on. Substituting Eqs. (8) through (12) into Eqs. (5) and (6) we obtain

$$\left[\mu \frac{\partial}{\partial z} + n(z) \, \sigma_p(E)\right] \Phi_p(z,E,\mu)$$

$$= n(z) \left[\sigma_p^{ex}(E+W) + \sigma_p^{i}(E+W)\right] \Phi_p(z,E+W,\mu)$$

$$+ n(z) \, \sigma^{01}(E+W) \, \Phi_H(z,E+W,\mu) \quad , \tag{13}$$

and,

$$\left[\mu \frac{\partial}{\partial z} + n(z) \, \sigma_H(E)\right] \Phi_H(z,E,\mu)$$

$$= n(z) \left[\sigma_H^{ex}(E+W) + \sigma_H^{i}(E+W)\right] \Phi_H(z,E+W,\mu)$$

$$+ n(z) \, \sigma^{10}(E+W) \, \Phi_p(z,E+W,\mu) \tag{14}$$

Here we have defined

$$\sigma_p(E) \equiv \sigma_p^{ex}(E) + \sigma_p^{i}(E) + \sigma^{10}(E) \tag{15}$$

and,

$$\sigma_H(E) \equiv \sigma_H^{ex}(E) + \sigma_H^{i}(E) + \sigma^{01}(E) \tag{16}$$

We notice that the elastic scattering terms drop out as a result of the forward-scattering assumption, and the coupling between the proton and H atom fluxes arise due to the charge-changing processes represented by σ^{10} and σ^{01}.

5.5 SOLUTIONS FOR THE FLUXES

Since the equilibriation of the incident proton flux occurs in the altitude region where energy loss is unimportant due to very low atmospheric density, we can analyze the precipitation problem in two stages. First, we neglect all energy losses and show that equilibration due to charge-changing processes is a direct consequence of Eqs. (13) and (14). We calculate the fractional compositions of protons and H atoms in the equilibrium mixture. Then, we solve the full transport equations for the fluxes taking the equilibrium fluxes as the given boundary values.

5.5.1 Equilibriating Fluxes

If we neglect all energy losses, Eqs. (13) and (14) reduce to

$$\left[\mu \frac{\partial}{\partial z} + n(z)\, \sigma^{10}(E)\right] \Phi_p(z,E,\mu) = n(z)\, \sigma^{01}(E)\, \Phi_H(z,E,\mu) \tag{17}$$

$$\left[\mu \frac{\partial}{\partial z} + n(z)\, \sigma^{01}(E)\right] \Phi_H(z,E,\mu) = n(z)\, \sigma^{10}(E)\, \Phi_p(z,E,\mu) \tag{18}$$

Adding the two equations we obtain

$$\mu \frac{\partial}{\partial z} \left[\Phi_p(z,E,\mu) + \Phi_H(z,E,\mu)\right] = 0 \quad , \tag{19}$$

which implies

$$\Phi_p(z,E,\mu) + \Phi_H(z,E,\mu) = \Phi_0(E,\mu) \tag{20}$$

where $\Phi_0(E,\mu)$ (for $-1 \le \mu < 0$) is the proton flux incident (at $z=\infty$) on the atmosphere. Equation (20) is just a statement of the conservation of flux. Inserting Eq. (20) into either (17) or (18), and defining an equilibriation depth τ_e as

$$d\tau_e = -(\sigma^{10} + \sigma^{01})\, n(z)\, dz \tag{21}$$

$$\Phi_p(\tau_e(z,E),E,\mu) = \Phi_0(E,\mu) \frac{\sigma^{01}}{\sigma^{10} + \sigma^{01}} \left(1 + \frac{\sigma^{10}}{\sigma^{10}} \exp(\tau_e/\mu)\right) \tag{22}$$

$$\Phi_H(\tau_e(z,E),E,\mu) = \Phi_0(E,\mu) \frac{\sigma^{10}}{\sigma^{10} + \sigma^{01}} \left(1 - \exp(\tau_e/\mu)\right) \tag{23}$$

for $-1 \leq \mu < 0$, and zero otherwise, since $\Phi_0(E,\mu) = 0$ for $0 < \mu \leq 1$, i.e., no particles are incident from below. According to Eqs. (22) and (23), the fluxes approach their respective equilibrium values, given by

$$\Phi_p^{eq}(E,\mu) = \frac{\sigma^{01}}{\sigma^{10} + \sigma^{01}} \Phi_0(E,\mu), \text{ for } -1 \leq \mu < 0 \quad , \tag{24}$$

and,

$$\Phi_H^{eq}(E,\mu) = \frac{\sigma^{10}}{\sigma^{10} + \sigma^{01}} \Phi_0(E,\mu), \text{ for } -1 \leq \mu < 0 \quad , \tag{25}$$

asymptotically.

For an isotropic incident proton flux, the hemispherically averaged values of the equilibriating fluxes are

$$\hat{\Phi}_p(\tau_e(z,E),E) = 2\pi \int_{-1}^{0} d\mu \, \Phi_p(\tau_e(z,E),E,\mu)/2\pi$$

$$= \hat{\Phi}_p^{eq}(E) \left[1 + \frac{\sigma^{10}}{\sigma^{01}} E_2(\tau_e(z,E))\right] \tag{26}$$

and,

$$\hat{\Phi}_H(\tau_e(z,E),E) = 2\pi \int_{-1}^{0} d\mu \, \Phi_H(\tau_e(z,E),E,\mu)/2\pi$$

$$= \hat{\Phi}_H^{eq}(E) \left[1 + E_2(\tau_e(z,E))\right] \tag{27}$$

Here,

$$\hat{\Phi}_p^{eq}(E) = \int_{-1}^{0} d\mu \, \Phi_p^{eq}(E,\mu) \quad , \tag{28}$$

$$\hat{\Phi}_H^{eq}(E) \equiv \int_{-1}^{0} d\mu\, \Phi_H^{eq}(E,\mu) \quad , \tag{29}$$

and, $E_2(x)$ is the second exponential integral function. In the upper atmosphere, the most effective charge-changing process are

$$H^+ + O \rightarrow H + O^+ \qquad (\sigma^{10})$$

$$H + O \rightarrow H^+ + O + e^- \qquad (\sigma^{01})$$

due to large abundance of oxygen atoms. We have calculated values of $\hat{\Phi}_p$ and $\hat{\Phi}_H$ as a function of altitude for an isotropic-Maxwellian incident proton flux, i.e.,

$$\Phi_O(E,\mu) = \left(\frac{Q_S}{2\pi E_o^3}\right) E \exp(-E/E_o) \quad , \text{ for } -1 \leq \mu < 0 \quad , \tag{30}$$

where Q_S is the total energy flux in the downward direction and E_o is the mean proton energy, using $\sigma^{10}(E)$ and $\sigma^{01}(E)$ of McNeal and Birely [1973] and using a model atmosphere [Jacchia, 1977; 1000°K]. We find that for E_o = 8 keV, for example, the fluxes attain their equilibrium values at approximately 290 km, i.e., $z_{eq} \approx 290$ km.

In the following precipitation analysis, we shall take $z=z_{eq}$ as the boundary, and solve Eqs. (13) and (14) with Φ_P^{eq} and Φ_H^{eq}, given by Eqs. (24) and (25) respectively, as the fluxes incident on the boundary.

5.5.2 Precipitating Fluxes

Transforming Eqs. (13) and (14) into equations in terms of the 'optical' depth τ, where

$$\tau = \tau(z,E) \equiv \sigma_p(E) \int_z^{z_{eq}} n(z')\, dz' \quad , \tag{31}$$

we obtain

$$\left(\mu \frac{\partial}{\partial \tau} - 1\right) \Phi_p(\tau(z,E),E,\mu) = - \frac{\tilde{\sigma}_p(E+W)}{\sigma_p(E)} \Phi_p(\tau(z,E+W),E+W,\mu)$$

$$- \frac{\sigma^{01}(E+W)}{\sigma_p(E)} \Phi_H(\tau(z,E+W),E+W,\mu) \quad , \tag{32}$$

and,

$$\left(\mu \frac{\partial}{\partial \tau} - 1\right) \Phi_H(\tau(z,E),E,\mu) = - \frac{\tilde{\sigma}_H(E+W)}{\sigma_p(E)} \Phi_H(\tau(z,E+W),E+W,\mu)$$

$$- \frac{\sigma^{10}(E+W)}{\sigma_p(E)} \Phi_p(\tau(z,E+W),E+W,\mu) \quad . \tag{33}$$

Here, we have introduced $\tilde{\sigma}_p = \sigma_p^{ex} + \sigma_p^i$, $\tilde{\sigma}_H = \sigma_H^{ex} + \sigma_H^i$ for brevity of notations, and assumed $\sigma_p(E) = \sigma_H(E)$, which is a fairly good approximation over the auroral energy range.

The formal solutions of Eqs. (32) and (33) are

$$\Phi_p(\tau,E,\mu) = \Phi_p^{eq}(E,\mu) \exp(\tau/\mu)$$

$$- \frac{\tilde{\sigma}_p(E+W)}{\sigma_p(E)} \int_o^\tau \frac{dt}{\mu} \Phi_p(b_{\shortparallel} t,E=W,\mu) \exp[(\tau-t)/\mu]$$

$$- \frac{\sigma^{01}(E+W)}{\sigma_p(E)} \int_o^\tau \frac{dt}{\mu} \Phi_H(b_{\shortparallel} t,E+W,\mu) \exp[(\tau-t)/\mu] \quad , \tag{34}$$

and

$$\Phi_H(\tau,E,\mu) = \Phi_H^{eq}(E,\mu) \exp(\tau/\mu)$$

$$- \frac{\tilde{\sigma}_H(E+W)}{\sigma_p(E)} \int_o^\tau \frac{dt}{\mu} \Phi_H(b_{\shortparallel} t,E+W,\mu) \exp[(\tau-t)/\mu]$$

$$- \frac{\sigma^{10}(E+W)}{\sigma_p(E)} \int_o^\tau \frac{dt}{\mu} \Phi_p(b_{\shortparallel} t,E+W,\mu) \exp[(\tau-t)/\mu] \quad , \tag{35}$$

for $-1 \leq \mu < 0$. Here $b_H(E) \equiv \sigma_p(E+W)/\sigma_p(E)$. Adding Eqs. (34) and (35) we obtain

$$\Phi_p(\tau,E,\mu) + \Phi_H(\tau,E,\mu) = \Phi_0(E,\mu)\ \exp(\tau/\mu)$$

$$- b_H(E) \int_0^\tau \frac{dt}{\mu} \left[\Phi_p(b_H t, E+W, \mu) + \Phi_H(b_H t, E+W, \mu)\right]$$

$$\times \exp\left[(\tau-t)/\mu\right] \qquad (36)$$

under the assumption $\sigma_p = \sigma_H$. In obtaining Eq. (36) we have used Eqs. (24) and (25). This equation for the combined flux can be solved by iteration procedure, which is equivalent to the multiple-scattering method used by Jasperse and Strickland [1979] in solving the auroral electron precipitation problem, and the complete solution is

$$\Phi_p(\tau,E,\mu) + \Phi_H(\tau,E,\mu) = \Phi_0(E,\mu)\ \exp(\tau/\mu) + \sum_{n=1}^{\infty} b_{n1}(E)$$

$$\times \Phi_0(E+nW,\mu) \left[H_n(\tau/\mu,E) - H_n(0,E)\ \exp(\tau/\mu)\right] \quad , \qquad (37)$$

for $-1 \leq \mu < 0$, and zero otherwise. In the above equation,

$$H_1(X,E) = a_{11}(E)\ \exp(b_{11}X) \quad , \qquad (38)$$

and the higher order H functions can be obtained from the recursion relation

$$\exp(-x)\ H_{n+1}(X,E) - H_{n+1}(0,E) =$$

$$- \int_0^X dx'\ \exp(-x')\ \left[H_n(b_{11}x', E+W) - H_n(0,E+W)\ \exp(b_{11}x')\right] \qquad (39)$$

so that

$$H_2(X,E) = a_{22}a_{21}\ \exp(b_{21}X) - a_{22}a_{11}\ \exp(b_{11}X) \quad , \qquad (40)$$

$$H_3(X,E) = a_{33}a_{32}a_{31}\ \exp(b_{31}X) - a_{33}a_{32}a_{11}\ \exp(b_{11}X)$$

$$- a_{33}a_{22}a_{21}\ \exp(b_{21}X) + a_{33}a_{22}a_{11}\ \exp(b_{11}X) \quad , \qquad (41)$$

etc. In the above formulae we have introduced the following definitions

$$b_{mn} = b_{mn}(E) \equiv \sigma_p(E+mW)/\sigma_p(E+(n-1)W) \quad , \tag{42}$$

$$a_{mn} = a_{mn}(E) = a_{mn}(E) \equiv \left[1 - b_{mn}(E)\right]^{-1} \quad . \tag{43}$$

That Eq. (37) solves (36) exactly can be verified by direct substitution and using the recursion relation (39).

Substituting Φ_{II} from Eq. (37) into Eq. (31) and doing integrations, we obtain

$$\begin{aligned}\Phi_p(\tau,E,\mu) = {} & \Phi_p^{eq}(E,\mu)\ \exp(\tau/\mu) \\ & + \frac{\sigma^{01}(E+W)}{\sigma_p(E+W)} \sum_{n=1}^{\infty} \Phi_0(E+nW,\mu) b_{n1}(E)\left[H_n(\tau/\mu,E) - H_n(0,E)\exp(\tau/\mu)\right] \\ & - \left(\frac{\tilde{\sigma}_p(E+W) - \sigma^{01}(E+W)}{\sigma_p(E+W)}\right) b_{11}(E) \int_0^{\tau} \frac{dt}{\mu}\ \Phi_p(b_{11}t, E+W, \mu) \\ & \times \exp[(\tau-t)/\mu]\end{aligned} \tag{44}$$

In doing the integrations we have used the recursion relation (39) and the definitions (42) and (43).

We now solve Eq. (44) by iteration, where the zeroth order iterate is

$$\begin{aligned}\Phi_p^{(0)}(\tau,E,\mu) = {} & \Phi_p^{Eq}(E,\mu)\ \exp(\tau/\mu) + \frac{\sigma^{01}(E+W)}{\sigma_p(E+W)} \sum_{n=1}^{\infty} \Phi_0(E+nW,\mu) \\ & \times b_{n1}(E)\ \left[H_n(\tau/\mu,E) - H_n(0,E)\ \exp(\tau/\mu)\right]\end{aligned} \tag{45}$$

After successive iteration, the resulting solution can be expressed in a closed form as:

$$\phi_p(\tau,E,\mu) = \phi_p^{(o)}(\tau,E,\mu) + \sum_{n=1}^{\infty} (R)_n \left[\phi_p^{Eq}(E+nW,\mu)\ b_{n1}(E) \right.$$

$$\times \left\{ H_n(\tau/\mu,E) - H_n(0,E)\ \exp(\tau/\mu) \right\} + \frac{\sigma^{01}(E+(n+1)W)}{\sigma_p(E+(n+1)W)} \sum_{m=n+1}^{\infty} \phi_o(E+mW,\mu)$$

$$\left. \times\ b_{m1}(E) \left\{ H_m(\tau/\mu,E) - H_m(0,E)\ \exp(\tau/\mu) \right\} \right] , \qquad (46)$$

where $\phi_p^{(o)}$ is given by Eq. (15), and

$$(R)_n = \left[\frac{\tilde{\sigma}_p(E+W) - \sigma^{01}(E+W)}{\sigma_p(E+W)} \right] \left[\frac{\tilde{\sigma}_p(E+2W) - \sigma^{01}(E+2W)}{\sigma_p(E+2W)} \right] \cdots\cdots \left[\frac{\tilde{\sigma}_p(E+nW) - \sigma^{01}(E+nW)}{\sigma_p(E+nW)} \right] , \qquad (47)$$

so that,

$$(R)_1 = \frac{\tilde{\sigma}_p(E+W) - \sigma^{01}(E+W)}{\sigma_p(E+W)} ,$$

$$(R)_2 = \left[\frac{\tilde{\sigma}_p(E+W) - \sigma^{01}(E+W)}{\sigma_p(E+W)} \right] \left[\frac{\tilde{\sigma}_p(E+2W) - \sigma^{01}(E+2W)}{\sigma_p(E+2W)} \right] , \quad \text{etc.}$$

Equations (37), (41) and (47) constitute the complete solution for the precipitating proton and hydrogen fluxes subject to the approximations that were made in the course of the analysis.

A few comments about the solutions are in order. The linear dependence of the fluxes at all altitudes on the incident flux is evident. The solutions yield no backscattered flux, i.e., $\phi=0$ for $0<\mu\leq 1$. The reason for this is that in the forward-scattering approximation elastic scattering terms drop out and no particles are scattered into the backward direction. Each factor in $(R)_n$ is a very small quantity (<0.06) over the auroral energy range, so that the sum in Eq. (46) converges extremely rapidly. For practical calculations, only the n=1 term in the sum should be quite sufficient.

5.6 HEMISPHERICALLY AVERAGED FLUXES, ENERGY DEPOSITION RATE AND IONIZATION RATE

In this section we give analytic expressions for various measurable quantities for an isotropic-Maxwellian incident proton flux as given in Eq. (30)

5.6.1 Hemispherically Averaged Fluxes

$$\begin{aligned}
\hat{\Phi}_p(\tau,E) &\equiv \int_{-1}^{0} d\mu\, \Phi_p(\tau,E,\mu) \\
&= \left(\frac{Q_S}{2\pi E_0^3}\right)\left[\left(\frac{\sigma^{01}(E)}{\sigma^{10}(E)+\sigma^{01}(E)}\right) E \exp(-E/E_0)\, E_2(\tau)\right. \\
&\quad + \frac{\sigma^{01}(E+W)}{\sigma_p(E+W)} \sum_{n=1}^{\infty} (E+nW)\exp(-(E+nW)/E_0)\, b_{n1} \\
&\quad \left.\times\left\{K_n(\tau,E) - H_n(0,E)\, E_2(\tau)\right\}\right] \\
&\quad + \left(\frac{Q_S}{2\pi E_0^3}\right) \sum_{n=1}^{\infty} (R)_n \left[\frac{\sigma^{01}(E+nW)}{\sigma^{10}(E+nW)+\sigma^{01}(E+nW)}\right. (E+nW) \\
&\quad \times \exp(-(E+nW)/E_0)\, b_{n1}\left\{K_n(\tau,E) - H_n(0,E)\, E_2(\tau)\right\} \\
&\quad \left. + \frac{\sigma^{01}(E+(n+1)W)}{\sigma_p(E+(n+1)W)} \sum_{m=n+1}^{\infty} (E+mW)\exp(-(E+mW)/E_0) b_{m1}\left\{K_m(\tau,E) - H_m(0,E) E_2(\tau)\right\}\right] .
\end{aligned} \tag{48}$$

and, according to Eq. (37),

$$\begin{aligned}
\hat{\Phi}_H(\tau,E) &= \left(\frac{Q_S}{2\pi E_0^3}\right)\left[E \exp(-E/E_0)\, E_2(\tau)\right. \\
&\quad \left. + \sum_{n=1}^{\infty} (E+nW)\exp(-(E+nW)/E_0)\, b_{n1}\left\{K_n(\tau,E) - H_n(0,E)\, E_2(\tau)\right\}\right] \\
&\quad - \hat{\Phi}_p(\tau,E) \quad ,
\end{aligned} \tag{49}$$

where $E_2(x)$ is the second exponential integral function defined by

$$E_2(X) = \int_1^\infty dt\ t^{-2} \exp(-xt) \quad , \tag{50}$$

and,

$$K_n(X,E) = \int_{-1}^{0} d\mu\ H_n(x/\mu,E) \tag{51}$$

It can be easily verified that the K-functions are the same as the H-functions with the exponential functions replaced by the E_2-functions everywhere.

5.6.2 Energy Deposition Rate

The energy deposition rate $\eta_E(z)$, defined as the energy deposited per unit volume per unit time by the precipitating fluxes, is given in plane-parallel geometry by

$$\eta_E(z) = 2\pi n(z) \int_0^\infty dE \int_{-1}^{0} d\mu\ \mu\ E\ \sigma_p(E) \frac{\partial}{\partial \tau} \left[\Phi_p(\tau,E,\mu) + \Phi_H(\tau,E,\mu)\right] \quad , \tag{52}$$

recognizing that $\partial\Phi(z)/\partial z = n(z)\sigma_p(E)\partial\Phi(\tau)/\partial\tau$. With the aid of Eq. (37) this becomes

$$\eta_E(\tau) = \left(\frac{Q_S}{E_0^3}\right) n(z) \int_{E_{min}}^\infty dE\ F\ \sigma_p(E) \left[E \exp(-E/E_0)\ E_2(\tau) + \sum_{n=1}^{\infty} (E+nW) \exp(-(E+nW)/E_0)\ b_{n1} \left\{L_n(\tau,E) - H_n(0,E)\ E_2(\tau)\right\}\right] \quad , \tag{53}$$

where

$$L_n(X,E) = \int_{-1}^{0} d\mu\ \mu \frac{\partial}{\partial x} H_n(x/\mu,E) \tag{54}$$

The rule for $L_n(X,E)$ is: find $\partial H_n(X,E)/\partial x$ and then replace the exponential functions by the E_2-functions everywhere. As discussed in the beginning of section 5.4, our analytic solutions for the fluxes, based on the forward-scattering approximation, are only valid for $E \geq E_{min}$. In doing the energy integral in Eq. (55) from E_{min} to ∞, instead of from 0 to ∞ which defines η_E, we lose contribution to the integral amounting a few percent for the auroral protons.

5.6.3 Ionization Rate

An important quantity describing the proton-hydrogen energy deposition in the auroral atmosphere is the ionization rate $\eta_i(z)$, defined as the number of electron-ion pairs created per unit volume per unit time. In proton auroras, in addition to the impact ionizations by fast protons and hydrogen atoms, an electron-ion pair is created at the end of each charge-changing cycle.

In plane-parallel geometry, $\eta_i(z)$ can be calculated from

$$\eta_i(z) = 2\pi\, n(z) \int_{E_{min}}^{\infty} \frac{dE}{W_S(E)} \int_{-1}^{0} d\mu\, \mu\, E\, \sigma_p(E)\, \frac{\partial}{\partial \tau} \left[\phi_p(\tau,E,\mu)+\phi_H(\tau,E,\mu)\right] \quad , \tag{55}$$

where $W_S(E)$ is the average energy expended in creating an electron-ion pair due to impact ionizations and charge-changing processes. Inserting Eq. (37) into (55) we obtain

$$\eta_i(z) = \left(\frac{O_S}{E_0^3}\right) n(z) \int_{E_{min}}^{\infty} \frac{dE}{W_S(E)}\, E\, \sigma_p(E) \left[E \exp(-E/E_0)\, E_2(\tau) + \sum_{n=1}^{(A)} (E+nW)\exp(-(E+nW)/E_0)\, b_{n1} \left\{ L_n(\tau,E) - H_n(0,E) E_2(\tau) \right\} \right] \quad . \tag{56}$$

The underlying assumption in writing Eq. (55) is that the energy deposited by the precipitating proton-hydrogen fluxes is entirely expended in producing electron-ion pairs. This is a reasonable assumption for $E - E_{min} \gtrsim 1$ keV, since the energy loss due to excitation processes is comparatively small owing to small cross sections.

We take for $W_S(E)$ the values calculated by Edgar et al [1973]. Typical values are 30, 27, 26, 27, 28 and 32 in eV for 1, 2, 5, 10, 20 and 50 keV proton energies, respectively. Because of charge-exchange a great number of ions are created at low energies leading to a dip in $W_S(E)$ below 10 keV proton energy.

We further point out that in evaluating the energy integrals in Eqs. (53) and (56), the integrals may be truncated at some E_{max}. When this is done the infinite sums terminate at a maximum value N given by $N = (E_{max}-E_{min})/W$.

5.7 PSEUDOPARTICLE METHOD

In the formulae of sections 5.6.1 through 5.6.3, W is ~30 eV and the incident auroral proton energies range from 1 to 60 keV. This means, the sums in the formulae extend to as many as 2,000 terms representing as many as 2,000 scatterings before an energetic proton loses all its energy. However, a good approximation to these large sums may be obtained by introducing the notion of pseudoparticles [Jasperse and Strickland, 1979]. A pseudoparticle is a particle which has a cross section $W/\tilde{W}$ times smaller than the real particle but has an average energy loss per inelastic collision $\tilde{W}/W$ times greater, where $\tilde{W} >> W$. In describing the energy precipitation in terms of the pseudoparticles, we simply replace σ by $\tilde{\sigma}$ and W by $\tilde{W}$ everywhere in Eqs. (48) through (56), i.e.

$$\sigma(E) \rightarrow \tilde{\sigma}(E) \equiv (W/\tilde{W})\, \sigma(E) \tag{57}$$

$$W \rightarrow \tilde{W} \equiv (\tilde{W}/W)\, W \tag{58}$$

We notice that under such transformations the energy loss function $L(E) \equiv W\sigma(E)$ remains unchanged; but, the number of terms in the sums is reduced by the factor $W/\tilde{W}$, i.e. $N \rightarrow N(W/\tilde{W})$.

Using the pseudoparticle method we have calculated the various quantities in sections 5.6.1 through 5.6.3. We have found that a converging answer can be obtained with a suprisingly small number of pseudoscatterings. For example, for an isotropic-Maxwellian incident proton flux with E_o = 8 keV only 10 pseudoscatterings (i.e. N=10) spanning the energy range from E_{min} = 2.5 keV to E_{max} = 57.5 keV yield good answers.

REFERENCES

Chamberlain, J. W., Physics of the Aurora and Airglow, Academic Press, New York, 1961.

Davidson, G. T., Expected spatial distribution of low-energy protons precipitated in the auroral zones, J. Geophys. Res., 70, 1061, 1965.

Eather, R. H., Auroral proton precipitation and hydrogen emissions, Rev. Geophys. 5, 207, 1967.

Edgar, B. C., W. T. Miles, and A. E. S. Green, Energy deposition of protons in molecular nitrogen and applications to proton auroral phenomena, J. Geophys. Res., 78, 6595, 1973.

Jacchia, L. G., Thermospheric temperature, density, and composition: New models, Smithson. Astrophys. Observ. Spec. Rept. 375, Cambridge, Mass., 1977.

Jasperse, J. R. and D. J. Strickland, Approximate analytic solutions for the primary auroral electron flux and related quantities, 1979.

McNeal, R. J. and J. H. Birely, Laboratory studies of collisions of energetic H^+ and hydrogen with atmospheric constituents, Rev. Geophys. Space Phys. 11, 633, 1973.

Vallance Jones, A., Aurora, D. Reidel, Dordrecht, Holland, 1974.

APPENDIX

We change over to spherical coordinates in velocity space using

$$v_\parallel = v\cos\theta,\quad v_\perp = v\sin\theta,\quad v_\perp\, dv_\perp dv_\parallel = v^2 dv\,\sin\theta\, d\theta$$

$$\frac{\partial F_{oh}}{\partial v_\parallel} = \frac{v_\parallel}{v}\,\frac{\partial F_{oh}}{\partial v};\quad \frac{\partial F_{oh}}{\partial v_\perp} = \frac{v_\perp}{v}\,\frac{\partial F_{oh}}{\partial v}$$

Then the expression for N_h becomes

$$N_h = \frac{2\pi e(\omega+i\nu_h)}{m}\sum_{n=-\infty}^{+\infty}\int_0^\infty dv\, v\int_0^\pi d\theta\,\sin\theta\,\frac{J_n^2(k_\perp v\sin\theta/\Omega)}{\omega+i\nu_h-k_\parallel v\cos\theta-n\Omega}\,\frac{\partial F_{oh}}{\partial v}$$

$$-\frac{4\pi e}{m}\int_0^\infty dv\, v\,\frac{\partial F_{oh}}{\partial v} \qquad (A1)$$

taking into account the identity $\sum_n J_n^2 = 1$. Let us consider the first integral. With the substitution

$$\frac{1}{\omega+i\nu_h-k_\parallel v\cos\theta-n\Omega} = -i\int_{-\infty}^0 d\tau\,\exp\{-i(\omega+i\nu_h-k_\parallel v\cos\theta-n\Omega)\tau\}$$

and using the addition theorem

$$J_0(a\sin b) = \sum_{n=-\infty}^{+\infty} J_n^2(a/2)\,\exp(2inb)$$

we can carry out the integration with respect to θ. The result is

$$I = -2i\int_0^\infty dv\,\frac{\partial F_{oh}}{\partial v}\int_{-\infty}^0 d\tau\,\frac{\sin Av}{A}\exp\{-i(\omega+i\nu_h)\tau\} \qquad (A2)$$

where $A = [k_\parallel\tau)^2 + (4k_\perp^2/\Omega^2)\,\sin^2\Omega\tau/2]^{1/2}$. Integrating by parts with respect to v we obtain

$$I = 2i\int_0^\infty dv\, F_{oh}(v)\int_{-\infty}^0 d\tau\,\cos Av\,\exp\{-i(\omega+i\nu_h)\tau\} \qquad (A3)$$

In the case $k_{\parallel}=0$, we can use the identity

$$\cos\{(2k_{\perp}v/\Omega)\ \sin\Omega\tau/2\} = \sum_{n=-\infty}^{+\infty} J_{2n}(2k_{\perp}v/\Omega)\ \exp(in\Omega\tau) \tag{A4}$$

and integrate with respect to τ. The result is

$$1 = -2 \sum_{n=-\infty}^{+\infty} \int_0^{\infty} dv\ F_{oh}(v)\ \frac{J_{2n}(2k_{\perp}v/\Omega)}{\omega+i\nu_h-n\Omega} \tag{A5}$$

Using (A5) in (A1) we get

$$N_h = \frac{4\pi e}{m} \int_0^{\infty} dv\ F_{oh}(V) \left[1 - (\omega+i\nu_h) \sum_{n=-\infty}^{+\infty} \frac{J_{2n}(2k_{\perp}v/\Omega)}{\omega+i\nu_h-n\Omega}\right] \tag{A6}$$

Following the procedure leading up to Eq. (A2), we get

$$D_h = 1 - \frac{2\pi\nu_h}{n_{oh}} \int_0^{\infty} dv\ v\ F_{oh}(v) \int_{-\infty}^{0} d\tau\ \frac{\sin Av}{A}\ \exp\{-i(\omega+i\nu_h)\tau\} \tag{A7}$$

Writing $\sin Av/A = \int_0^{v} dv'\ \cos Av'$ and performing the integration with respect to τ using Eq. (A1), we obtain

$$D_h = 1 - \frac{4\pi}{n_{oh}} \sum_{n=-\infty}^{+\infty} \frac{i\nu_h}{\omega+i\nu_h-n\Omega} \int_0^{\infty} dv\ v\ F_{oh}(v) \int_0^{v} dv'\ J_{2n}(2k_{\perp}v'/\Omega) \tag{A8}$$

Finally, using

$$\int_0^{x} dx'\ J_{2n}(x') = \sum_{p=0}^{\infty} J_{2n+2p+1}(x)$$

we obtain

$$D_h = 1 - \frac{4\pi\Omega}{k_{\perp}n_{oh}} \sum_{n=-\infty}^{+\infty} \frac{i\nu_h}{\omega+i\nu_h-n\Omega} \int_0^{B} dv\ v\ F_{oh} \sum_{p=0}^{\infty} J_{2n+2p+1}(2k_{\perp}v/\Omega) \tag{A9}$$

TABLE 1

Maximum collisionless growth rate γ_m, collisional damping rate ω_i, and other parameters of the upper hybrid instability as a function of altitude, for $B_o = 0.35G$. Here, $K_\perp (= k_\perp v_o/\Omega)$ and $K_\perp/K_{||} (= k_\perp/k_{||})$ refer to the values for which maximum growth rate is obtained.

Altitude (km)	ω_{pe}/Ω	$\omega_H (s^{-1})$	$\nu_m (s^{-1})$	$\omega_i (s^{-1})$	$\gamma_m (s^{-1})$	$K_\perp$	$K_\perp/K_{||}$
120	3.22	2.08×10^7	1.5×10^3	8.16×10^2	1.49×10^3	8.8	19.5
130	3.68	2.35×10^7	7.53×10^2	4.02×10^2	4.04×10^3	10.1	45.5
140	4.3	2.72×10^7	4.26×10^2	2.24×10^2	4.68×10^3	10.8	21.4
170	5.16	3.24×10^7	1.14×10^2	0.6×10^2	4.79×10^4	12.8	41.1

TABLE 2

Maximum collisionless growth rate γ_m, collisional damping rate, and other parameters of the electron cyclotron instability as a function of altitude, for B_o = 0.35G.

Altitude (km)	$\omega/\Omega=n$	$\omega_{pe}/\Omega=(n^2-1)^{\frac{1}{2}}$	$\nu_m(s^{-1})$	$\omega_i(s^{-1})$	$\gamma_m(s^{-1})$	k_m
100	2	1.73	1.4×10^4	4.37×10^3	1.48×10^2	4.6
110	3	2.83	4.32×10^3	1.2×10^3	7.28×10^3	5.8
130	4	3.87	7.53×10^2	2.0×10^2	2.89×10^4	7.1


MED
8